Integrated Multi-Mission Ocean Altimeter Data for Climate Research TOPEX/Poseidon, Jason-1 and OSTM/Jason-2 User's Handbook

Version 2

Table of Contents

Table of Figures

Brian Beckley	SGT, Inc.
Richard Ray	NASA/GSFC
Simon Holmes	SGT, Inc.
Nikita Zelensky	SGT, Inc.
Frank Lemoine	NASA/GSFC
Xu Yang	SGT, Inc.
Shannon Brown	JPL/Caltech/NASA
Shailen Desai	JPL/Caltech/NASA
Gary Mitchum	University of South Florida
Jessica Hausman	JPL/Caltech/NASA

Introduction

Maintenance and improvements to the fidelity of the TOPEX/Poseidon, Jason-1 and Jason-2/OSTM (TPJAOS) Sea Surface Height Climate Data Record (SSH CDR) is a continuous effort through the research activities of the Ocean Surface Topography Science Team (OSTST). As further advancements and/or re-calibrations are made to any of the correction parameters or models, the TPJAOS product is recalculated with the most accurate algorithms sanctioned by the OSTST. Notification and details of revisions to the TPJAOS will be provided and announced by the Physical Oceanography Distributed Active Archive Center (PODAAC) and displayed at this site http://podaac.jpl.nasa.gov/Integrated_Multi-Mission_Ocean_AltimeterData. Users will be notified of revisions to ensure they are consistently up to date.

Since the last quarterly release of TPJAOS v1.0 which spanned through cycle 144 of Jason-2, a number of algorithm revision/improvements prompted the release of a revised version 2 that extends to the most current Jason-2 repeat cycle. Most notable was the release of the Jason-2 version D Geophysical Data Record (GDR_D) replacing the initial version T (GDR_T) heritage, and advances in the Precise Orbit Determination (POD) that would provide improved realizations of the Time Variable Gravity (TVG) for all three missions.

In summary the following revisions were incorporated in the development of TPJAOS version 2.0:

- GSFC std1204 orbit replacing std1007
- Jason-2 GDR heritage based on GDR_D replacing GDR_t
- Jason-1 sea state bias, revision of model currently on GDR_C (see Appendix II)
- Jason-2 sea state bias, revision of model currently on GDR_D (see Appendix II)
- Jason-1 "pseudo time tag bias" application
- Revised inter-mission bias estimates

The following sections of this report detail these and other revisions to the SSH record and any subsequent impacts to validation results and mean sea level estimates. Users are referred to the Version 1.0 handbook (ftp://podaac.jpl.nasa.gov/allData/merged_alt/preview/L2/docs/) for algorithm specifications that have remained unchanged.

1.0 General Structure Characteristics

The MEaSURE's TPJAOS v2.0 sea surface height (SSH) anomaly product is a multi-mission data set comprised of TOPEX/Poseidon (T/P), Jason-1, and OSTM (Jason-2) altimeter data integrated to form a single SSH Climate Data Record (CDR). Altimeter data from the multi-mission Geophysical Data Records (GDRs) are interpolated to a common reference orbit facilitating direct time series analysis of the geo-referenced SSH. The baseline v2.0 file is comprised of 748 10-day repeat cycles:

Cycle 1 – 355 T/P (cycles 1 – 355)

356 – 582 Jason-1 (cycles 13 -239)

583 – 748 OSTM (cycles 1 – 166)

As future OSTM cycles become available the direct access structure of the file allows new data to be appended. All inter-mission biases have been applied to provide a seamless transition throughout the current 20- year record.

Each 10-day repeat cycle is comprised of 127 revolutions. Each revolution has 6745 along-track locations spanning the equatorial ascending node (Figure 1).

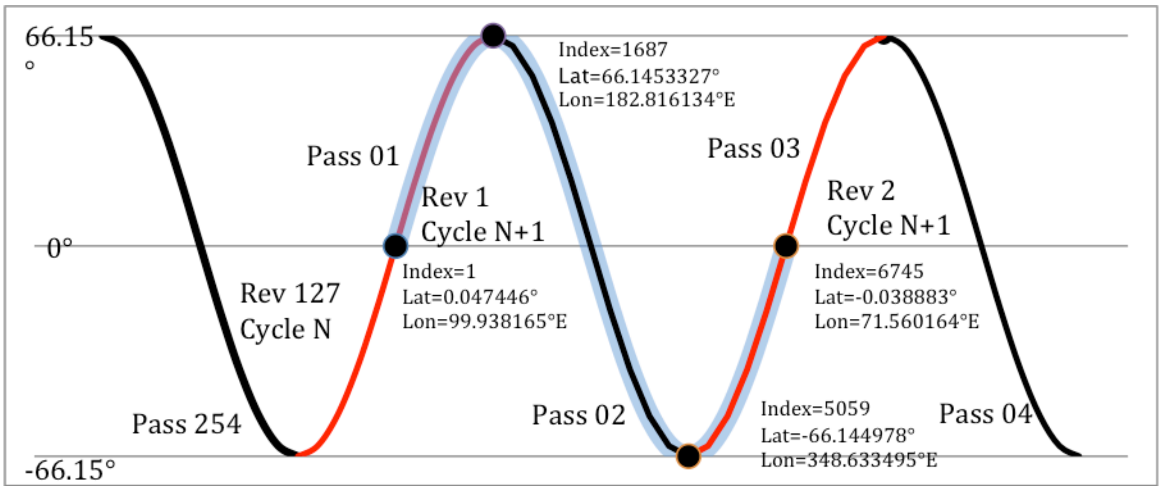

Figure 1: GDR convention of ascending odd numbered passes (solid red lines) and descending even numbered passes (solid black lines) total 254 passes/repeat cycle. The MEaSURE's product convention is based on 127-revolutions/repeat cycle. Revolution #1 is shown (blue shading overlay) with reference orbit lat/lon coordinates indicated for first and last geo-reference index, and for index at maximum and minimum latitude.

Each SSH data record is a SSH time series at a specific geo-referenced location defined by revolution number and along-track index. A 3-dimensional directory (rev#, index, cycle) permits direct access of individual locations at specific times (i.e. temporal and spatial sub-sampling). Auxiliary files provide time, mean sea surface reference, terrain type, bathymetry, proximity to coast, and SSH quality assessments (flag word) at each geo-referenced location.

1.1 Geo-referenced 1Hz SSH

Construction of the 1Hz geo-referenced SSH is achieved by sampling the GDR high-rate SSH (10Hz for T/P and 20Hz for Jason-1 and OSTM) from contiguous 1Hz samples that align with the reference index location, and the time at the reference location derived from the GDR (figure 2).

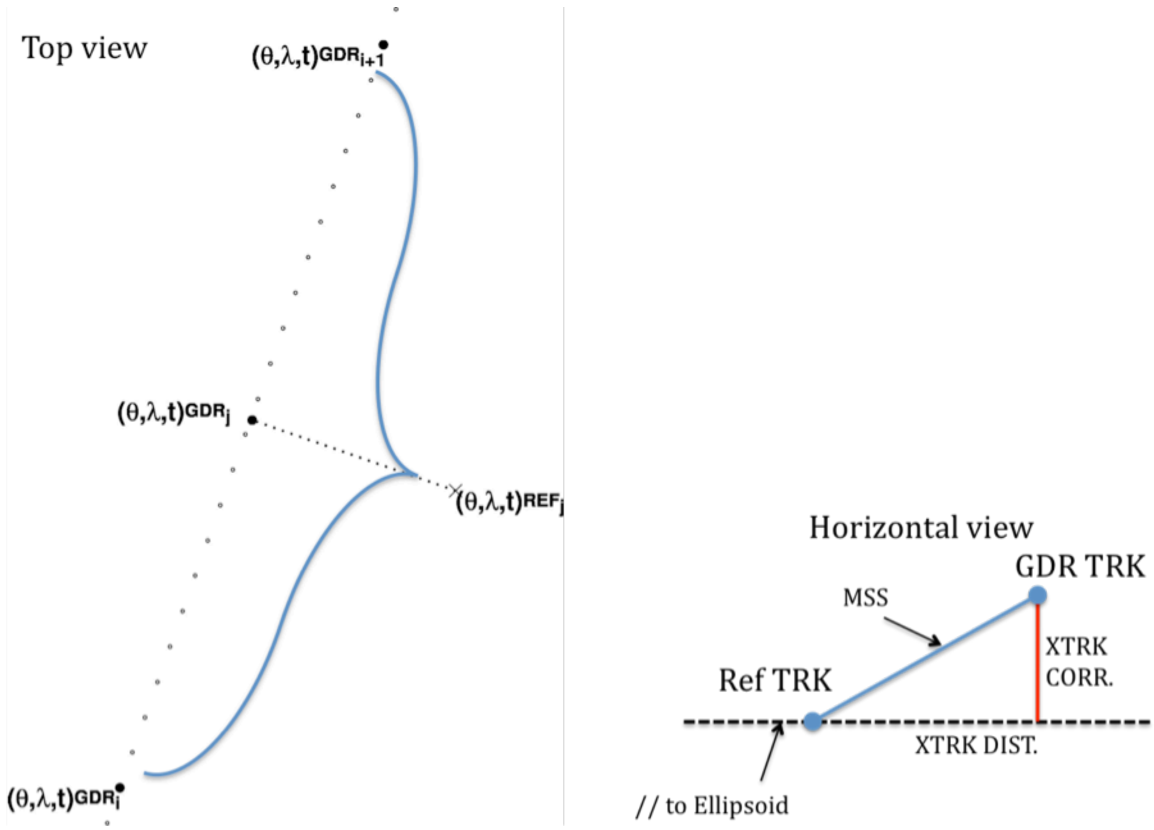

Figure 2: 1Hz SSH constructed at reference orbit locations (REF $_j$) is achieved by re-sampling high-rate SSH from contiguous 1Hz GDR SSH (GDR $_i$ and GDR $_{i+1}$) evaluated at mid-point GDR $_j$.

Satellites can deviate from the nominal orbit ground track by up to ± 1 km. To correct for this, a Mean Sea Surface [MSS] model can be used to effect a cross-track transformation between the along-track SSH and the corresponding SSH on the reference orbit. Towards this end, the normal projected onto the GDR groundtrack from the reference location provides the cross-track distance. The product of the cross-track distance and the local slope of the DTU10 MSS provide the cross-track gradient correction (Brenner et al, 1990) applied to account for local MSS gradients. The regression fit of the high-rate SSH is performed employing the GDR routine g1071 (TOPEX Ground System Science Algorithm Specification, 1991). Additional constraints require a minimum number of high-rate SSH (6 for T/P, and 16 for Jason-1 and OSTM), and a minimum number of high-rate SSH on each side of the midpoint (2 for T/P and 7 for Jason-1 and OSTM). The standard deviation of the high-rate residuals with respect to the resultant 1Hz average fit is computed and incorporated in the SSH quality assessment flag word (see table 2).

1.2 Construction of the Corrected SSH Anomaly

$SSH_{uncorrected}$ = Orbit (GSFC std1204) - $Range_{corrected}$

$SSH_{corrected}$ = $SSH_{uncorrected}$ - Dry Troposphere Delay

- Wet Troposphere Delay

- Solid Earth Tide

- Ocean Tide

- Ocean Load Tide

- Pole Tide

- Ionosphere Delay

- Sea State Bias (SSB) Delay

- Atmospheric Load (IB)

- Cross-track gradient

+ inter-mission bias

$SSH_{anomaly}$ = $SSH_{corrected}$ - DTU10 mean sea surface

T/P $Range_{corrected}$ = $Range_{\text{net instrument applied}}$ + Center of Mass correction (Cg)

Jason-1 $Range_{corrected}$ = $Range_{\text{net instrument applied}}$ + pseudo time tag bias

Jason-2 $Range_{corrected}$ = $Range_{\text{net instrument applied}}$

The GDR heritage for each mission:

- T/P MGDR_B (Benada, 1997)
- Jason-1 GDR_C (Picot et al., 2008)
- OSTM GDR_D (OSTM/Jason-2 products handbook, December 2011)

Origination of individual range and geophysical corrections applied to the SSH for each mission is detailed in table 1. Corrections employed that were directly obtained from GDR are identified by their parameter name as in handbook in bold italics. Many of the altimeter corrections present on the mission GDRs have been recomputed to take advantage of more recent and accurate models and to insure consistency across missions. The development and implementation of replacement or revised correction parameters are explained in sections below.

Table 1: Heritage of range and geophysical corrections applied to the SSH for each mission.

Mission/ Correction parameter	TOPEX	Poseidon	Jason-1	OSTM
Orbit	GSFC std1204	GSFC std1204	GSFC std1204	GSFC std1204
Range Ku	Cg ***CG_Range_Corr***	Cg ***CG_Range_Corr***	pseudo_time tag_bias *	pseudo time tag bias *
Dry Trop.	ECMWF Interim Re-analysis	ECMWF Interim Re-analysis	ECMWF operational	ECMWF operational
Wet Trop.	TMR replacement product	TMR replacement product	JMR replacement product	GDR_D AMR ***Wet_trop_rad***
Ocean Tide	GOT4.9	GOT4.9	GOT4.8	GOT4.8
Load Tide	GOT4.7	GOT4.7	GOT4.7	GOT4.7
Pole Tide	Wahr, 1985 ***H_Pol***	Wahr, 1985 ***H_Pol***	Wahr, 1985 ***pole_tide***	Wahr, 1985 ***pole_tide***
Solid Earth Tide	*Cartwright and Tayler* [1971] and *Cartwright and Edden* [1973] ***H_Set***	*Cartwright and Tayler* [1971] and *Cartwright and Edden* [1973] ***H_Set***	*Cartwright and Tayler* [1971] and *Cartwright and Edden* [1973] ***solid_earth_tide***	*Cartwright and Tayler* [1971] and *Cartwright and Edden* [1973] ***solid_earth_tide***
Ionosphere	Dual-frequency ***Iono_Corr***	Doris/GIM ***Iono_Dor***	Dual-frequency ***iono_corr_alt_ku***	Dual-frequency ***iono_corr_alt_ku***
Sea State Bias	Non- parametric collinear residuals (Tran, et. al , 2010)	Parametric BM4 crossover residuals (Gaspar et al 1994) ***EMB_Gaspar***	Non-parametric collinear residuals (Tran et. al, 2010, 2012)	Non-parametric collinear residuals (Tran et al 2012)
Cross-track gradient	DTU10	DTU10	DTU10	DTU10

Atmospheric Load (IB)	Dynamic Atmospheric Correction (DAC)	Dynamic Atmospheric Correction (DAC)	ECMWF operational + MOG2D hi-frequency ***inv_bar_corr + hf_fluctuations_corr***	ECMWF operational + MOG2D hi-frequency ***inv_bar_corr + hf_fluctuations_corr***
Inter-mission bias	7.2 mm (Alt A/ B)	N/A	-86.9 mm wrt TOPEX	-14.2 mm wrt TOPEX

* Psuedo time tag bias for Jason-1 and Jason-2

The explanation for the root cause of what has been referred to as the "pseudo-datation" time tag bias has been found to be essentially an algorithm error. It is due to altimeter algorithms time tagging measurements based upon emitted versus received pulse. For Jason-2 this error in GDR-T processing algorithms was corrected in the GDR-D by correcting the error in the processing algorithms. Thus there is no need for an explicit empirical "pseudo-datation bias" parameter for Jason-2 GDRD. The same error in the processing of Jason-1 GDR-C altimeter data exists. At the time that Jason-1 GDR-C standards were set, it was known that a time tag bias existed, but the source of the time tag bias was then not known. Therefore a "pseudo-datation" bias was provided separately as an explicit correction parameter in Jason-1 GDR-C. The current accounting for this time tag bias in Jason-1 GDR-C is to correct the time tag during the interpolation procedure of the GSFC replacement orbit:

Let *t(GDRC)* = Time tag of altimeter data on GDR-C.
Let *t* = correct altimeter time tag that accounts for algorithm error.
Then $t = t(GDRC) - 18/2058.513239 + 2.0*alt/c$
alt = satellite altitude above ellipsoid
c = speed of light
Use *t* to determine orbit.

A SSH anomaly with respect to the DTU10 mean sea surface (Andersen, 2010) is computed if all correction fields are available (i.e. various conventions used throughout not set to default value). If one or more of the corrections applied are outside accepted nominal ranges, a quality assessment flag word bit is set to indicate the less than optimal quality. This rationale allows maximum retention of coastal and inland water observations that may otherwise be edited as “blunders” by open ocean standards. Table 2 lists the nominal ranges for each correction that with few exceptions follows the GDR handbook recommendations.

Table 2: Nominal ranges for individual correction parameters. Quality flag word bit #6 (see SSH Quality Flag Word description below) is set if any single correction parameter is outside nominal range.

Correction parameter	Nominal range
Dry Troposphere	> -2600 mm and < -1900 mm
Wet Troposphere	≥ 0 mm and < -600 mm
Ocean Tide	> -5 m and < + 5 m
Load Tide	> -150 mm and < +150 mm
Pole Tide	≥ -100 mm and ≤ +100 mm
Solid Earth Tide	≥ -1000 mm and ≤ +1000 mm
Sea State Bias	> -600 mm and ≤ 0 mm
Altimeter derived wind speed	≥ 0 m/s and < 25 m/s
Atmospheric load	≥ -1000 mm and ≤ +1000 mm
Cg	≥ -20 mm and ≤ +20 mm
Psuedo time tag bias	≥ -10 mm and ≤ +10 mm

1.3 SSH Quality Flag Word

For each 1Hz geo-referenced SSH anomaly, a flag word is assigned to further assess the quality of the resultant SSH determination and provide the capability for tailored edit strategies for particular user applications.

Bit 0 : blank

Bit 1 : = 0 Dual-frequency altimeter measurement

= 1 Single frequency altimeter measurement

Bit 2 : = 0 depth ≥ 200 meters

= 1 depth < 200 meters

Bit 3 : = 0 proximity to land ≥ 50 km

= 1 proximity to land < 50 km

Bit 4 : = 0 Sigma H of fit < 15 cm (< 20 cm for Poseidon-1)

= 1 Sigma H of fit ≥ 15 cm (≥ 20 cm for Poseidon-1)

Bit 5 : = 0 high rate SSH sampled from two contiguous 1Hz data observations

= 1 high rate SSH sampled from single 1Hz observation

Bit 6 : = 0 all SSH corrections within nominal range

= 1 one or more of SSH corrections outside nominal range

Bit 7 : = 0 Cross Track Distance < 1.0 km.

= 1 Cross Track Distance ≥ 1.0 km.

Bit 8 : = 0 Cross Track Slope < 10 cm/km.

= 1 Cross Track Slope ≥ 10 cm/km.

Bit 9 : = 0 Significant Wave Height < 8 m and > 0 m(Ku band)

= 1 Significant Wave Height ≥ 8 m or = 0 m(Ku band)

Bit 10 : = 0 Sea ice not detected

= 1 Sea ice detected

Bit 11 : = 0 No rain contamination detected

= 1 Possible rain contamination detected.

Bit 12 : = 0 Sigma0 ≥ 6 db and ≤ 27 db (Ku band)

= 1 Sigma0 < 6 db or > 27 db (Ku band)

Bit 13 : = 0 Attitude (Att_Wvf) ≥ 0 and ≤ 0.3 degrees (T/P)

= 0 off_nadir_angle_ku_wvf ≥ -.09 deg^2 and ≤ +.09 deg^2

= 1 Attitude (Att_Wvf) < 0 or > 0.3 degrees (T/P)

= 1 off_nadir_angle_ku_wvf < -.09 deg^2 or > +.09 deg^2

Bit 14 : = 0 radiometer observation NOT suspect (tmr_bad set=0)

= 1 radiometer observation suspect (tmr_bad set > 0)

Bit 15 : = 0 GOT4.8 minus FES04 tide models differ by ≤ 2 cm.

= 1 GOT4.8 minus FES-4 tide models differ by > 2 cm.

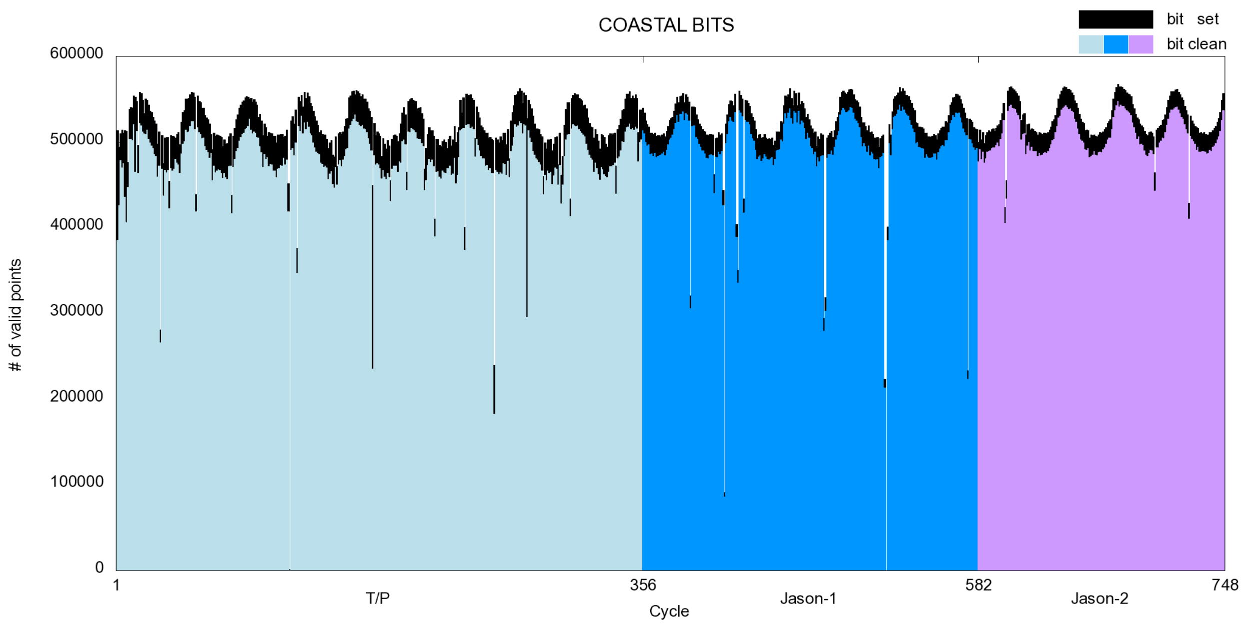

Figure 3: Approximately 5% of valid (not set to default value of 32767) open ocean SSH anomalies are edited based on an edit strategy that requires bits 4-14 pass (i.e. equal 0). Bits 2,3, and 15 are not checked thus retaining coastal observations.

2.0 GSFC Replacement Orbit

2.1 The satellite orbit height correction

Accurate orbit determination is central to the computation of the altimeter-derived surface elevation observation. The orbit defines the geocentric reference for the satellite altimeter sea surface measurement. Orbit accuracy and consistency are essential not only to the altimeter measurement accuracy across one mission, but also for the seamless transition between missions (Beckley, et. al, 2004). The analysis of altimeter data for TOPEX/Poseidon (TP), Jason-1 (J1) and Jason-2 (J2) requires that the orbits for all three missions be in a consistent reference frame, and calculated with the best possible standards to minimize error and maximize the data return from the time series, particularly with respect to the demanding application of consistently measuring global sea level change. This multi-mission altimetry time series can provide unprecedented insight into long-period ocean/atmosphere coupling needed for better understanding climate change. There are very demanding 1-cm radial orbit accuracy and cross-mission consistency objectives required to meet this goal (Cazenave et al., 2009, Ablain et al., 2009, Beckley et al., 2010). The orbit is also essential to calibrating the altimeter range, other altimeter corrections such as the sea state bias, and the inter-mission range bias. Such MEaSURE's altimeter bias corrections are based on the same orbits as are used for the geocentric height correction described in this section.

Insuring the highest accuracy and consistency of the satellite orbit is a critical component of the MEaSURE's task. Foremost is the application of improved GSFC replacement orbits that would tie multiple missions to a common well-defined geodetic reference frame (Beckley et al., 2007). Orbit testing at GSFC, has shown progressive improvement with increasingly refined POD modeling. Since 2009 GSFC has released three orbit series based on progressively improved POD standards: 1) the ITRF2005-based std0905, 2) the ITRF2008-based std1007 used previously in the MEaSURE's v1.0 product, 3) the latest std1204 standards implemented in the MEaSURE's v2.0 product. The std0905 SLR/DORIS dynamic radial orbit accuracies have been accessed at 1.5 cm (Lemoine et al., 2010, Zelensky et al., 2010). Since then improvements to POD modeling have led to orbit improvement in the ITRF2008-based std1007, and further improvement in std1204. This latest standard, std1204, offers three principal improvements over std1007: 1) time variable gravity (TVG) modeling, 2) updates to the SLR/DORIS ITRF2008 complements and SLR bias management, 3) reduction of solar radiation pressure (SRP) error in the Jason-1/2 orbit through estimation of once per rev (opr) acceleration parameters every 12-hours. Table 3 outlines the models used in the std1204 standards. Tests have shown using low degree/order gravity coefficients (tvg4x4) estimated every 7-days from SLR and DORIS tracking (Lemoine et al., 2012) improve the satellite orbits across the TP, J1, and J2 missions. Although both GRACE-derived and the recent SLR/DORIS derived TVG models improve the orbits from about 2005, the GRACE-derived TVG models do not accurately project back into the TOPEX era (Zelensky et al, 2012). The std1204 TVG model includes a set of 4x4 annual, semi-annual, and linear gravity coefficient terms fit to the tvg4x4 gravity coefficient time series estimated from SLR/DORIS (Lemoine et al., 2012).

SLR/DORIS precise orbits were generated for the entire T/P, Jason-1, and OSTM (Ocean Surface Topography Mission or Jason-2) mission time series based on the most recent std1204 POD standards (Table 3). Tests using the latest std1204 standards show improvement of the T/P, Jason-1, and Jason-2 orbits over the previous std1007 series (Table 4). Std1204 shows an overall reduction in SLR/DORIS and independent Crossover residuals, and also an increase in tracking coverage since 2008 due to new station updates to ITRF2008 (Table 4). Figure 4 illustrates the std1204 orbit improvement relative to std1007 using independent crossover residual data. The observed jump in improvement from TP to J1 is due to the reduction in SRP error, the trends due to TVG modeling improvement. These revisions to the precise orbit provide the geodetic consistency requirement necessary to tie T/P, Jason-1, and OSTM.

Table 3. GSFC POD Model Standards February 2013: std1204 **(**changes from std1007 in red**)**	
Reference frame and displacement of reference points	
SLR	SLRF2008 – update to IGN ITRF2008 complement and bias management
DORIS	DPOD2008 – update to IGN ITRF2008 complement
Earth tide	IERS2003
Ocean loading	GOT4.8 all stations
Tidal CoM &EOP	GOT4.7; VLBI high frequency terms
EOP	IERS Bulletin A daily (consistent with ITRF2008)
Precession / Nutation	IAU2000
Gravity	
Static	GOCO2s_fit2. GOCO2S 5x250 static field (Goiginer et al., 2011) + 4x4 static coefficients least squares fit to GSFC 19-year tvg4x4 time series.
Time varying	Depending on the coefficient 4X4 annual, semi-annual and linear terms fit to the GSFC 19-year **tvg4x4** time series, 18.6-yr term fit to C_{20} + 05x20 annual terms from GRACE.
Atmospheric	ECMWF, 50x50@6hrs
Tides	Got4.8 20x20 (ocean); IERS2003 (Earth)

Satellite Surface Forces and attitude			
Albedo /IR	Knocke-Ries-Tapley (1988)		
Atmospheric drag	MSIS86		
Radiation pressure	**TOPEX**	**Jason-1**	**Jason-2**
	tuned 8-panel	UCL	Jason-1 8-panel
Radiation scale coeff.	C_R = 1.0	C_R = 1.0	C_R = 0.945 (retuned)
Attitude	Nominal Yaw; quatern. off-nominal	Nominal Yaw	Quaternions
Tracking data and parameterization			
Tracking data	SLR/DORIS (Jason1 DORIS corrected for SAA)		
Troposphere model	SLR: Mendez-Pavlis; DORIS: GPT+Saastamoinen+GMF; est. scale to wet		
Parameterization	Drag/8 hrs + opr along & cross-track (/24 hrs TP) (/12 hrs J1, J2) + DORIS time bias /arc; 10-day arc dynamic solution		
Antenna reference	**TOPEX**	**Jason-1**	**Jason-2**
SLR	LRA model	tuned offset	pre-launch
DORIS	pre-launch	pre-launch	pre-launch
SLR/DORIS weight	10-cm / 2-mm/s	10-cm / 3-mm/s; down-weight 14 SAA stations	10-cm / 2-mm/s

Table 4. Evaluation of std1204 SLR/DORIS orbit performance for TP, J1, and OSTM

Mission	orbit	average points		average RMS residuals		
		DORIS	SLR	DORIS (mm/s)	SLR (cm)	Xover * (cm)
TP cycles 13-446	std1007	56437	5380	0.4978	1.653	5.611
Jan 1993 – Oct 2004	std1204	56429	5386	0.4955	1.589	5.605
J1 cycles 1-259	std1007	111502	4101	0.3851	1.051	5.540

Jan 2002 – Jan 2009	std1204	110959	4103	0.3696	0.843	5.507
J2 cycles 1-160 (xover to cycle 145) Jul 2008 – Nov 2012	std1007	142906	4358	0.3643	1.094	5.543
	std1204	168165	4576	0.3785	0.912	5.470
* altimeter crossover data are independent						

The stability and accuracy of the orbit time series is affected by errors in the force models, the terrestrial reference frame (TRF), and errors in the tracking data and measurement models. The std0905 TP SLR/DORIS orbits have been determined to an accuracy of 1.5 to 2 cm over the 14-year mission, and the J1 and J2 SLR/DORIS dynamic orbits to accuracy close to 1-cm (Lemoine et al., 2010, Zelensky et al., 2010). Std1007 and std1204 offer further improvements to orbit accuracy. Since the latest TP orbits are considerably more accurate than the 2-3cm orbits present on the MGDR_B (Marshal et al., 1995), orbit differences will largely show GDR orbit error. So for example, a global error trend of 0.34 mm/yr in the TP GDR orbits is removed due to the much greater stability of the ITRF2008 realization (Figure 4a). Although the orbit difference rates between std1204-std1007 are neglibible over the TP and J1 periods of interest (Figure 4b), such is not the case for Jason-2 (Figures 4b, 4c). The trend in the J2 orbit differences is believed to be due to progressive increase in TVG modeling error in std1007. Although std1204 represents an improvement in TVG modeling over std1007, the issue of TVG modeling error is far from resolved. For example, comparison with the J2 JPL GPS RLSE11a (jpl11a) reduced-dynamic orbit, believed to be less sensitive to the effects of gravity error (Bertiger et al., 2010) , significantly differs between std1204 (Figure 5a) and the the GDRD orbits (Figure 5b) which employ the state of the art GRACE-based TVG modeling (Cerri et al, 2010). As expected, the differences between the GDR_D and std1204 orbits are also significant (Figure 5c). So it is seen error in TVG modeling remains an open issue. TVG modeling improvement remains under investigation at GSFC

Although the J1/J2 GDR_C POD models are consistent with the std1007 GSFC standards, and the orbits are of comparable accuracy (Cerri et al., 2010), spectral analysis of the J1/J2 orbit difference time series sampled every 10-days at geographic locations show a 118-day term due to differences in modeling the solar radiation pressure (Figure 6). Much of the SRP error has been reduced through the estimation of opr parameters spaced every 12 rather than 24 hours. Comparison with the J2 jpl11a orbit, believed insensitive to SRP error (Bertiger et al., 2010), shows the reduction of this error when estimating the opr parameter every 12-hours (Figure 7). Solar radiation pressure model improvement based on a more physical model for J1/J2 remains under investigation at GSFC.

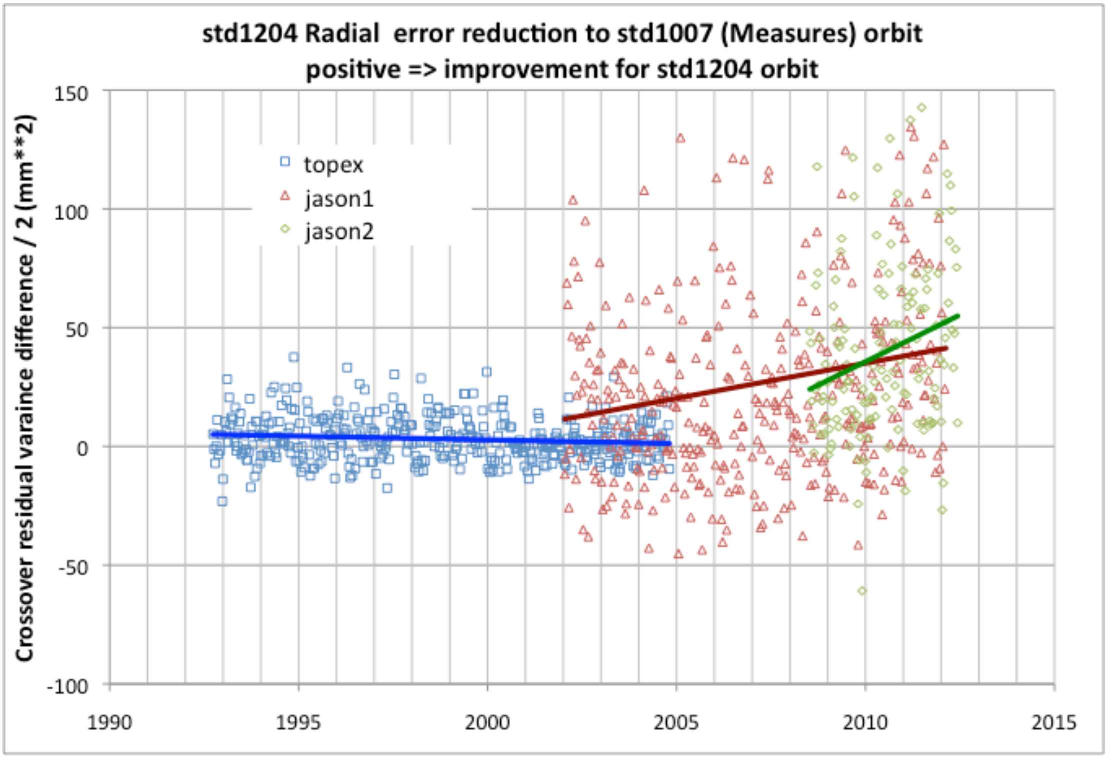

Figure 4. Std1204 radial orbit accuracy relative to std1007 using crossover data.

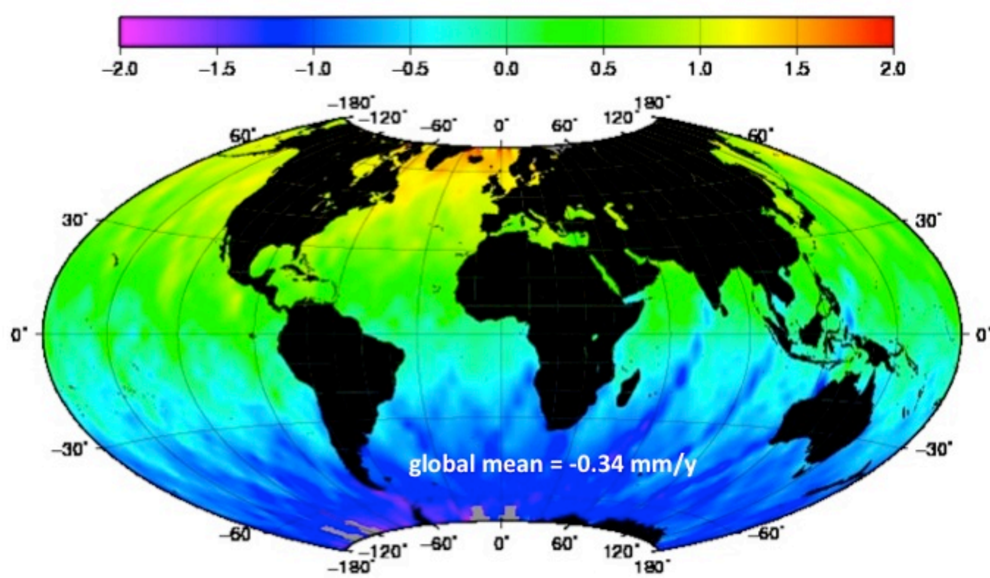

Figure 4a: T/P (cycles 11 – 340) linear rates (mm/yr) derived from std1007-GDR radial orbit differences.

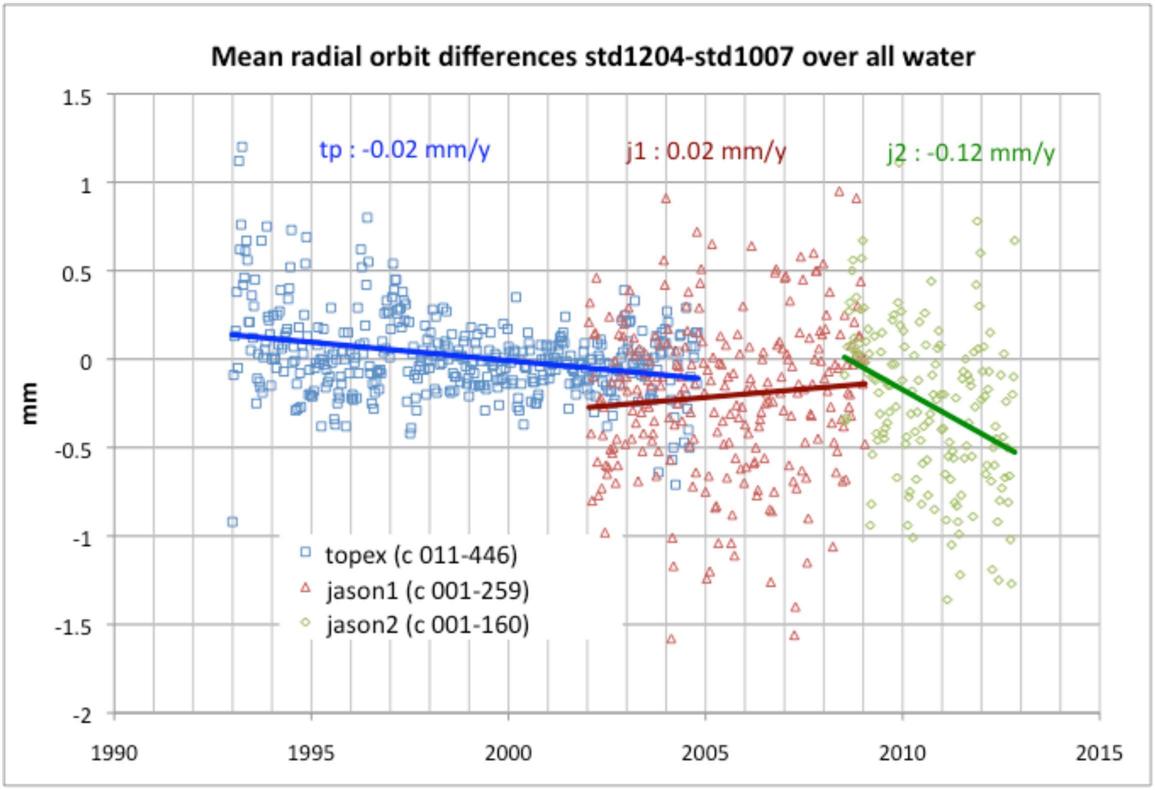

Figure 4b. Mean radial std1204-std1007 orbit differences/cycle over water.

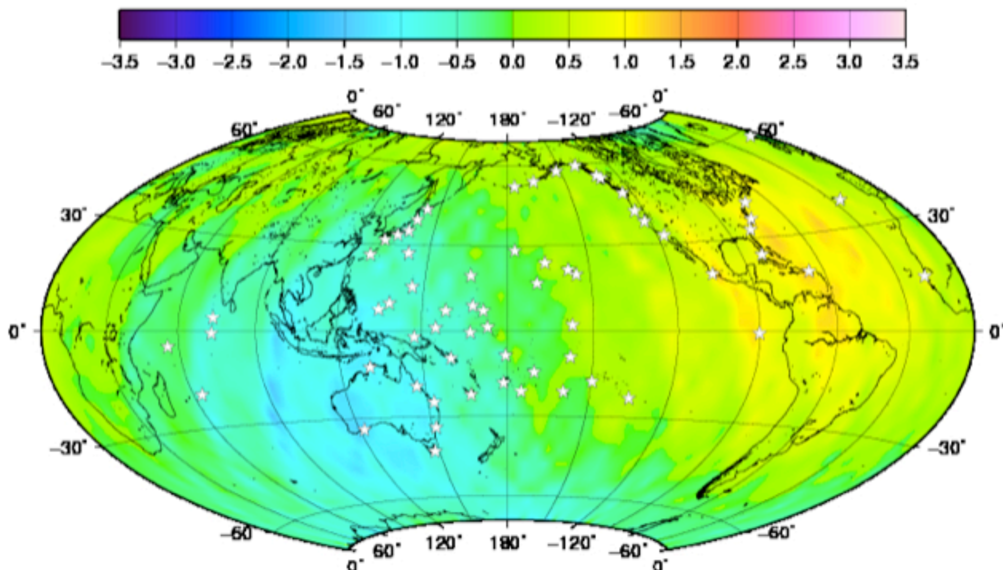

mm/y	global	water	TG
mean	-0.06	-0.13	-0.13
std dev	0.66	0.67	0.80

Figure 4c. Std1204 – std1007 radial orbit difference linear rates (mm/y) estimated over July 2008 – November 2012 (cycles 1-160) after removing annual, semi-annual, and 118-day terms.

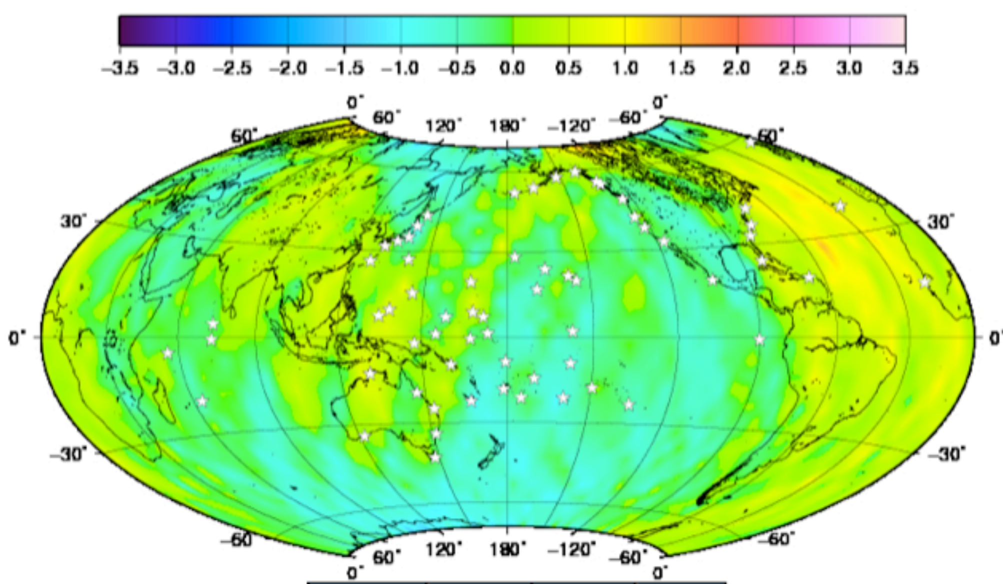

mm/y	global	water	TG
mean	-0.04	-0.13	0.13
std dev	0.71	0.72	0.74

Figure 5a: Jason-2 std1204 – jpl11a radial orbit difference linear rates (mm/y) estimated over July 2008 – July 2012 (cycles 1-149) after removing annual, semi-annual, and 118-day terms.

.

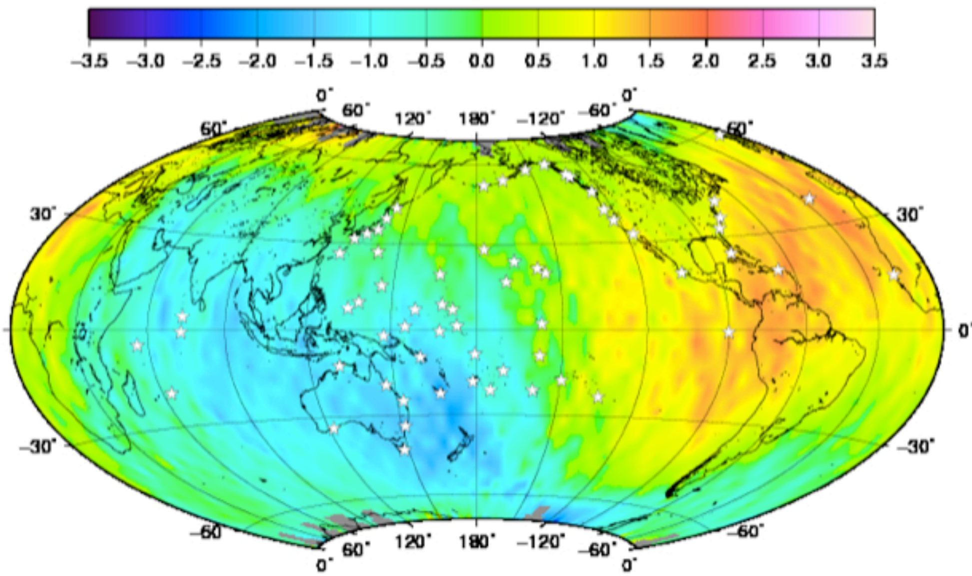

mm/y	global	water	TG
mean	-0.05	-0.15	-0.21
std dev	0.92	0.94	0.90

Figure 5b: Jason-2 GDR_D – jpl11a radial orbit difference linear rates (mm/y) estimated over July 2008 – July 2012 (cycles 1-149) after removing annual, semi-annual, and 118-day terms.

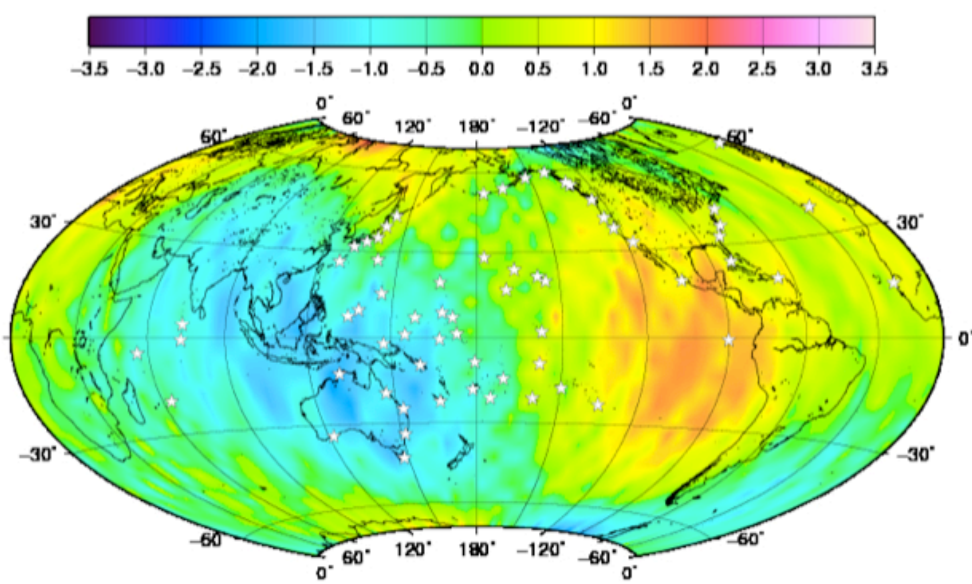

mm/y	global	water	TG
mean	0.02	-0.03	-0.29
std dev	1.04	1.06	1.05

Figure 5c: Jason-2 GDR_D – std1204 radial orbit difference linear rates (mm/y) estimated over July 2008 – July 2012 (cycles 1-149) after removing annual, semi-annual, and 118-day terms.

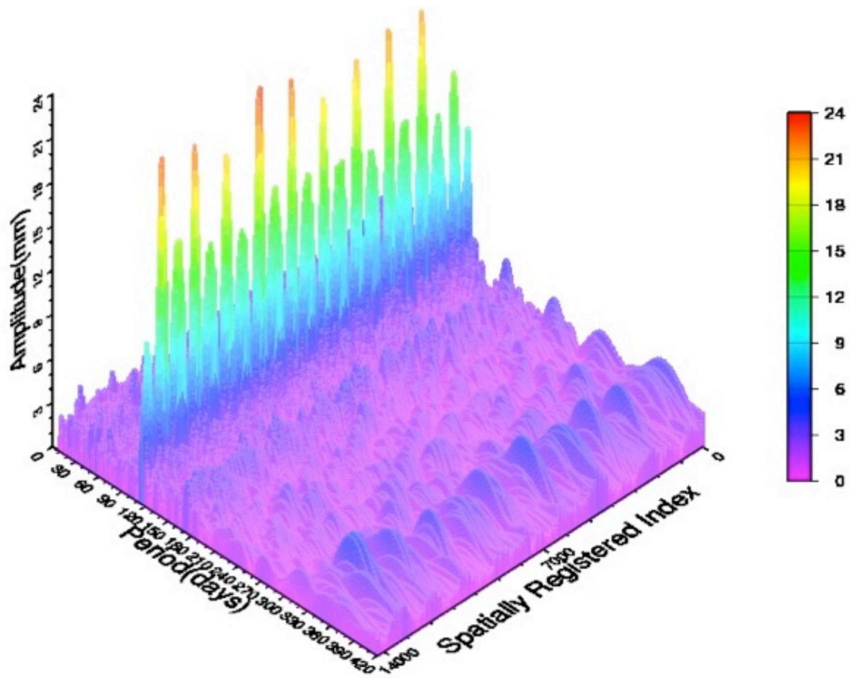

Figure 6: Spectral analysis of Jason-1+Jason-2 std1007-GDR radial differences (mm) sampled at geographically registered locations.

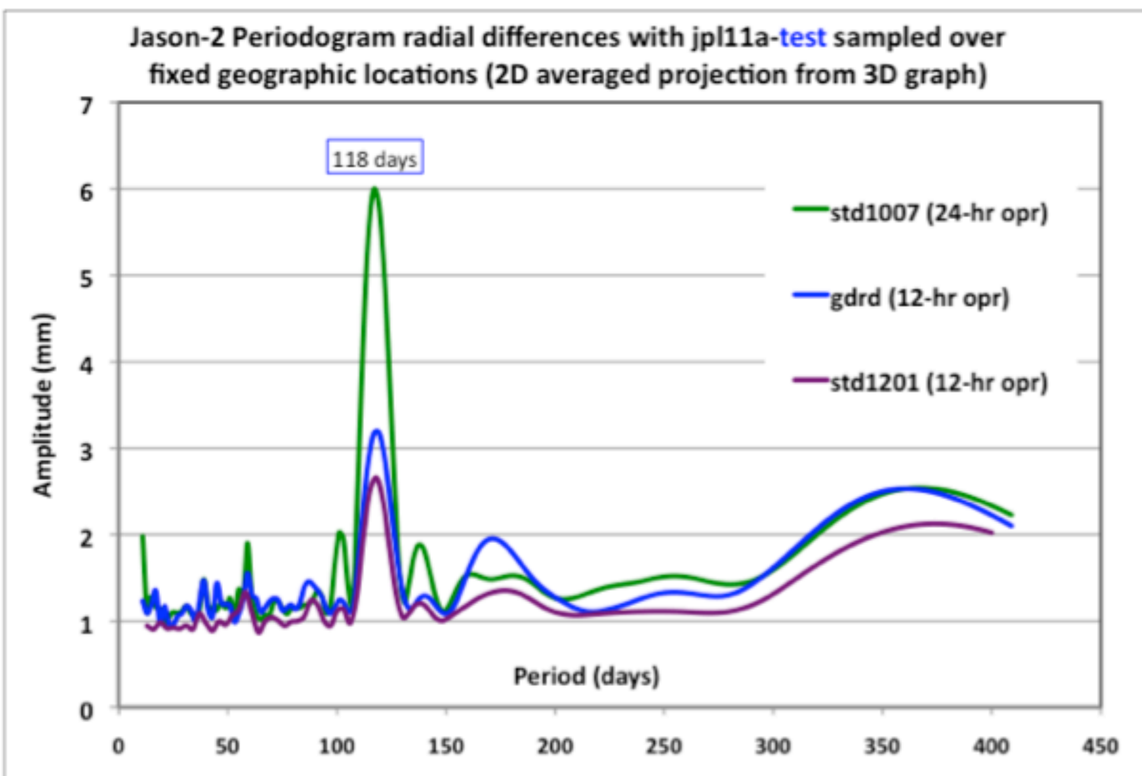

Figure 7: Solar Radiation Pressure error reduced with 12-hr opr estimates.

3.0 Inter-mission biases

3.1 Sea State Bias

In an effort to adhere to inter-mission consistency and provide a homogeneous SSH time series, the non-parametric (NP) sea state bias models that have evolved over time based on the works of Gaspar et al., 1998, 2002, Labroue et al., 2004, and most recently Tran et al., 2010&2012 have been employed to correct for sea state bias effects on the TOPEX, Jason-1&2 altimeters. Continuous improvements to these empirical based models has been due in part to improved POD strategies based on consistent geophysical modeling strategies and a single terrestrial reference frame adopted across all missions (Lemoine, et al, 2010), adoption of a consistent ground reprocessing strategy (4-parameter Maximum Likelihood Estimator (MLE4) re-tracking, Amarouche et al., 2004), improved atmospheric load corrections (Carrère and Lyard, 2003), and revised 2-parameter wind speed algorithms specifically tuned for TOPEX (Gourrion et al., 2002), and Jason-1 (Collard, 2004) altimeters. The specific SSB tables implemented for each mission are identified in Appendix II and can be obtained from AVISO.

A collaborative effort with Dr. Ngan Tran from CLS has produced non-parametic (NP) solutions for TOPEX (Side A and B) derived from collinear SSH residuals based on revised GSFC std0809 ITRF2005 (Eigen-GL04c) replacement orbits, and current correction algorithms outlined in Table 2 (Tran et al, 2010). Improved agreement between TOPEX and Jason-1 (see Figure 9) is realized with the application of the NP model as compared to results based on a revised parametric model derived from crossover residuals (Beckley, et al 2010). Comparison of the two models via SSH collinear differences shows an approximate +3mm Side A bias and -4mm Side B bias and an annual signature of 1mm in amplitude of the mean difference (Figure 8). Rectification of the approximate overall 7mm Side A/B bias is accomplished by comparing the altimeter derived SSH variations to the height variations from a near global network of tide gauges (see Tide Gauge Validation section below).

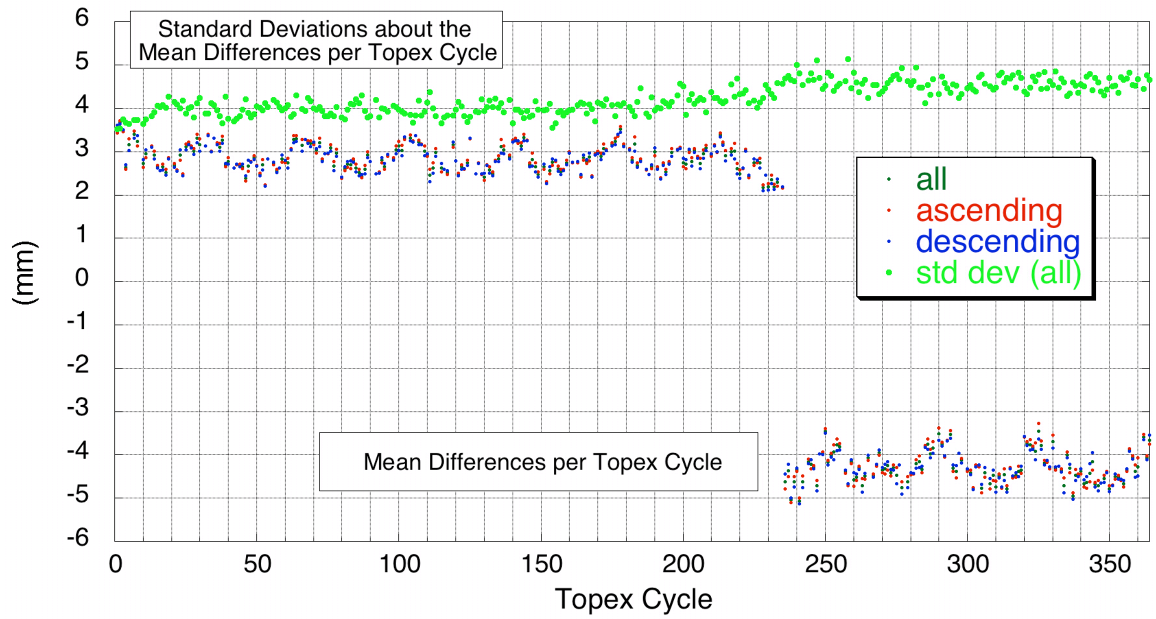

Figure 8: Mean differences of sea surface height between heights based on parametric versus non-parametric sea state bias solutions reveals separate biases for TOPEX Side A (cycles 1-235) and for Side B (cycles 236-364).

3.2 Jason-1 and Jason-2 Verification Phase Results

A critical component to providing credible mean sea level estimates from integrated multiple altimeter missions is the accurate determination of inter-mission biases. The verification campaigns during the roughly first 6 months of the Jason-1 and Jason-2 missions provided essential near-simultaneous altimeter observations that would enable the seamless transition from T/P to Jason-1 to Jason-2.

Figures 9 and 10 show the estimated global mean bias between TOPEX/Jason-1 and Jason-1/Jason-2 respectively derived from regional mean variations of the SSH collinear differences of the near-coincident measurements over the entire period of the verification phase(s). All pertinent range and geophysical corrections are applied in order to identify and isolate any regional residual differences/errors attributed to any remaining unavoidable inter-mission inconsistencies. Both figures show some expected regional variance in the estimate of the global mean bias estimate, though each estimate has a very normalized distribution of SSH mean residuals with a standard deviation barely exceeding 2 mm.

Note the inter-mission biases of 86.9 mm and 14.2 mm for Jason1&2 respectively are with respect to an already adjusted TOPEX (Side B with respect to Side A). The only revision to the T/P SSH series was the GSFC replacement orbit. Figure 11 shows the mean differences per cycle between the std1204 and std1007 orbits. Based on this analysis of the orbit differences between Side A and Side B, no additional adjustment to the 7.2 mm bias applied to TOPEX Side B is deemed necessary. A small reduction of ~2mm in the Jason-1/TOPEX inter-mission bias (86.9 mm versus 89.0 mm in previous version 1) can be attributed to the revised Jason-1 sea state bias algorithm (Tran et al., 2012, see Appendix II).

More pronounced is the ~15 cm OSTM/TOPEX bias reduction (14.2 mm versus 166.9 mm in previous version 1) due to the identification of range biases by the Jason-2 project team and subsequent application in the revised GDR_D. As stated in Section 3.1.1.2 in the OSTM/Jason-2 Products Handbook: "There are 2 main components which contribute to this bias of the order of 17.0 cm observed from global analyses or from the in-situ CalVal sites, 1) A lack of accuracy of the altimeter PRF (Pulse Repetition Frequency) that is applied today in the ground segment (truncation effect). If applied correctly, the JA2 range will be shorten by 25 mm, so increasing the absolute bias to 19.5 cms, and 2) A wrong antenna reference point for the computation of the Jason-2 range. If applied correctly, the JA2 range will be increased by 180 mm, thus decreasing the absolute bias to about 1.5 cm. These two errors (Jason-2 PRF value and antenna reference point) are corrected in the Jason- 2 GDR_D products version" (OSTM/Jason-2 Products Handbook, CNES: SALP-MU-M-OP-15815-CN, Issue 1 rev 8, December 1, 2011). A further revision to the Jason-2 GDR_D sea state bias (Ku band, MLE4 retracking) also contributes to the revised inter-mission bias estimate (Tran, et al., 2012, see Appendix II).

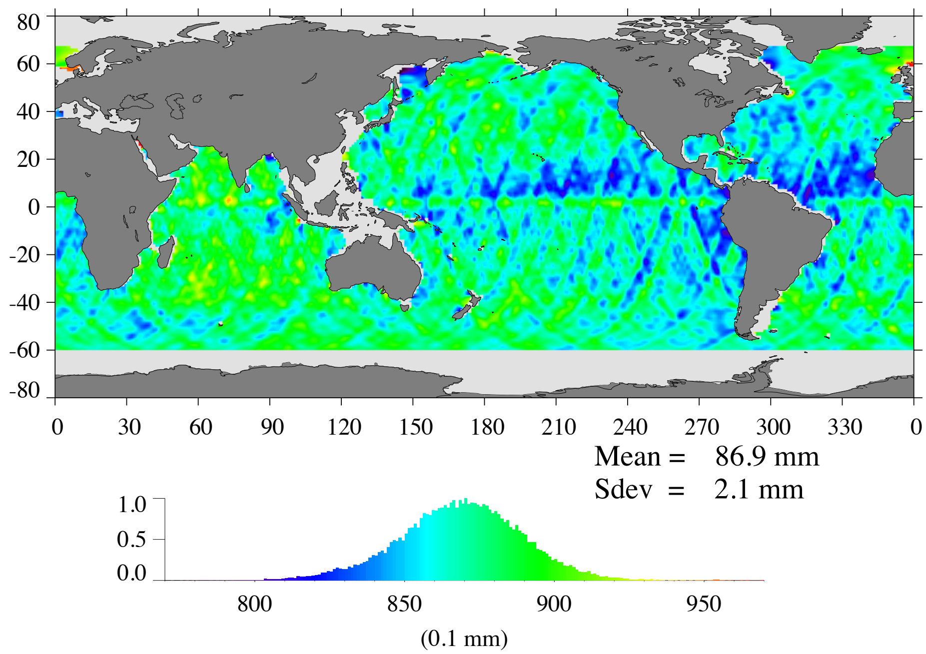

Figure 9: Jason-1 minus TOPEX (adjusted Alt B) inter-mission bias is estimated from averaged SSH collinear residuals during the Jason-1 verification phase. Color scale is exactly +/- 1cm about estimated mean.

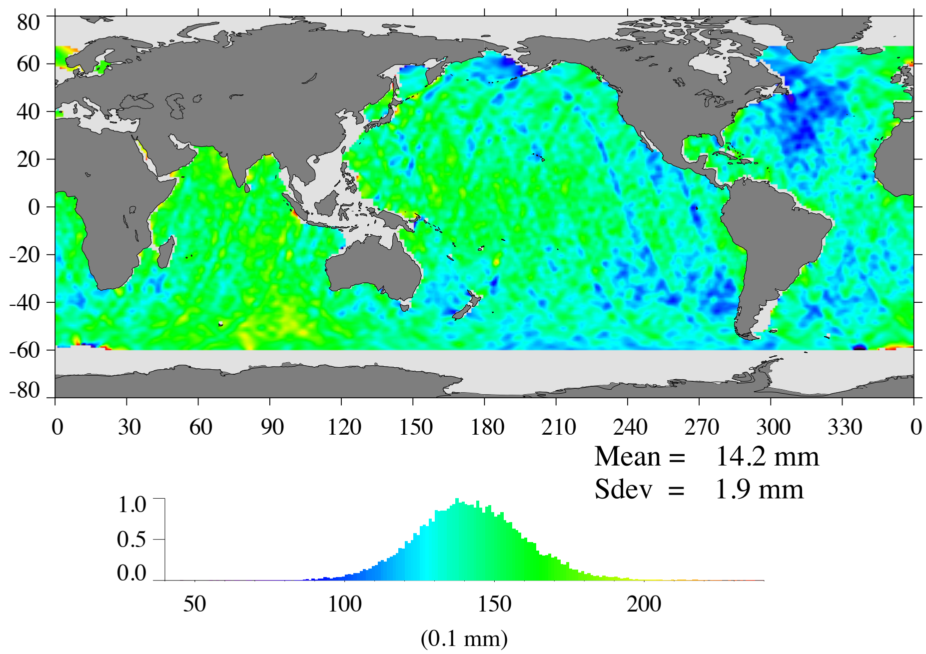

Figure 10: Jason-2 minus Jason-1 (adjusted to TOPEX) inter-mission bias is estimated from averaged SSH collinear residuals during Jason-2 verification phase. Color scale is exactly +/- 1cm about estimated mean.

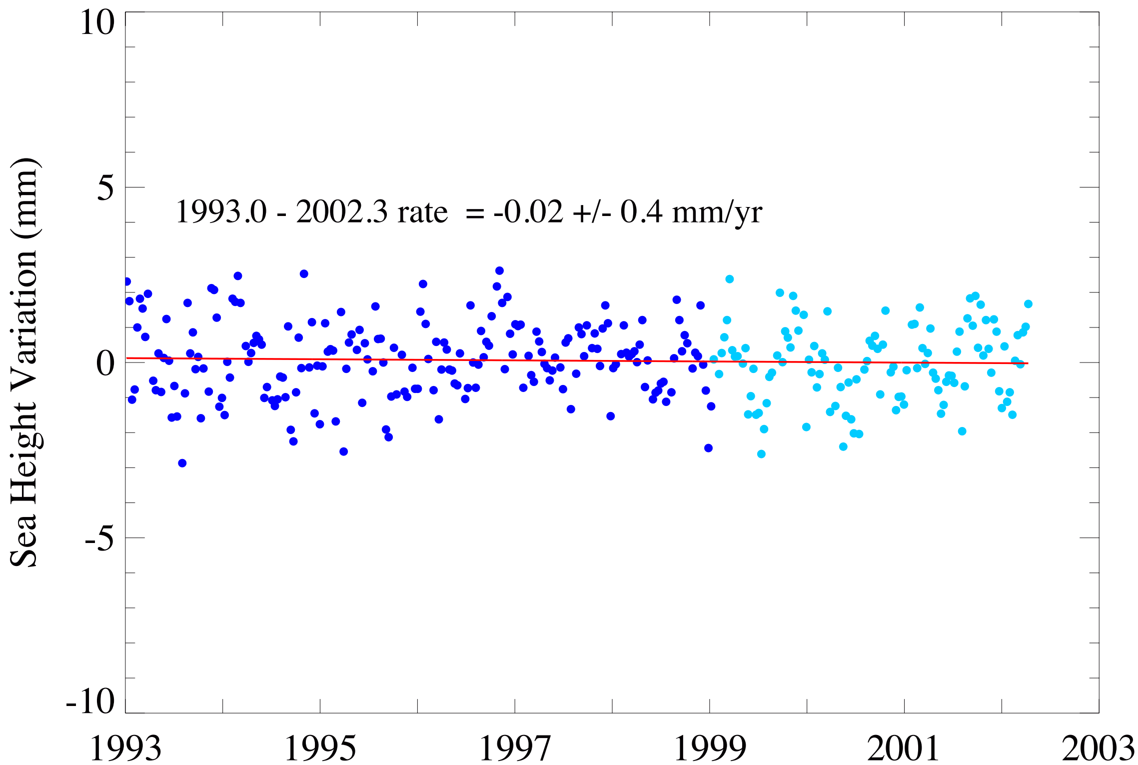

Figure 11: Mean orbit differences between GSFC replacement orbit std1204 and std1007 indicate that an additional TOPEX AltA/AltB bias adjustment is not warranted.

3.3 Tide Gauge Validations

Validation procedures are regularly performed by Prof. Gary Mitchum by comparing altimeter derived SSH variations to height variations measured from a global network of tide gauges (Mitchum, 2000). From the beginning of the TOPEX/Poseidon (T/P) mission, methods to estimate altimeter drift from comparisons with the global tide gauge network have continuously evolved, (for example, as the SSH time series approached two decades, questions about the handling of long period tides, particularly the Msf and Mf components, were raised and we adapted our methods appropriately) first in a research mode with NASA funding (primarily the T/P and OST SWTs and later from MEaSUREs), and later becoming more general and operationally-oriented.

Validation results shown here are based on the current near-global network of 64 sites. Work is nearly completed that will expand the network to 84 sites, providing much needed information in the Southern Hemisphere (Figure 12). The largest uncertainty in estimated rates derived from the gauges arises from land motion at the sites. Vertical land motion corrections based on GPS series from Wöppelmann, et al., 2009 have been implemented and updated based on revised ITRF realizations.

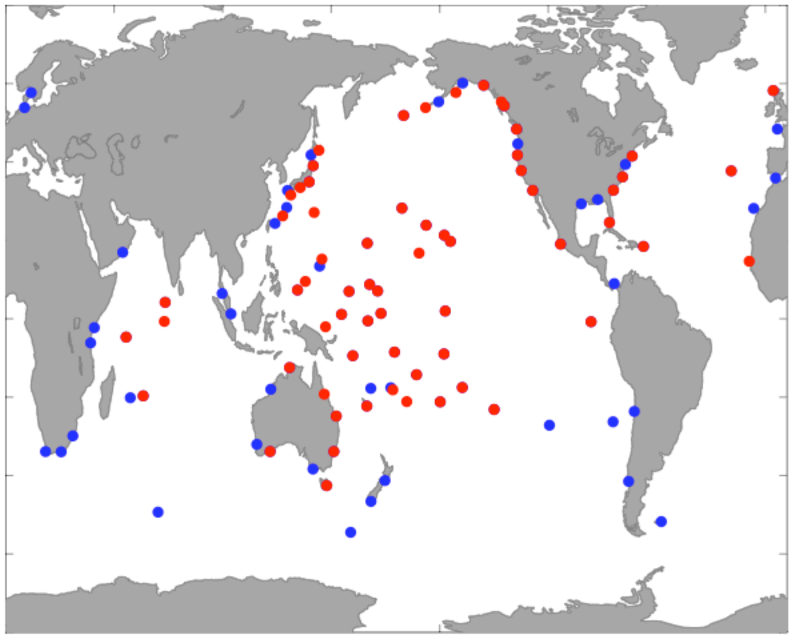

Figure 12: Current network of 64-tide gauge sites (red dots); soon to be expanded to 84 sites (additional blue dots).

The tide gauge validation analysis tools currently in place evaluates and monitors within-mission stability, and provides an assessment of inter-mission bias estimates (Nerem, et al., 2010, Leuliette and Scharoo, 2010, Beckley et al., 2010). As shown in figures 9 and 10 TOPEX/Jason-1 and Jason-1/Jason-2 inter-mission biases can be evaluated globally by direct SSH collinear differencing benefiting from the dedicated verification phases. The TOPEX Side A and Side B altimeters are treated as if separate missions as is noted in the independent evaluation of the sea state bias for each altimeter. There is no Side A/B coincident overlapping data available thus we are reliant on the tide gauge network to estimate this particular "inter-mission" bias. Figure 13 shows an estimated Side A/B bias of -7.2 mm resultant to differences in mean variations to a common TOPEX reference. Note that Side B is first tied to Jason-1 via the accurate inter-mission bias derived from the Jason-1 verification phase (Figure 9) to provide a longer SSH series resulting in a more stable rate estimate (0.18 mm/y).

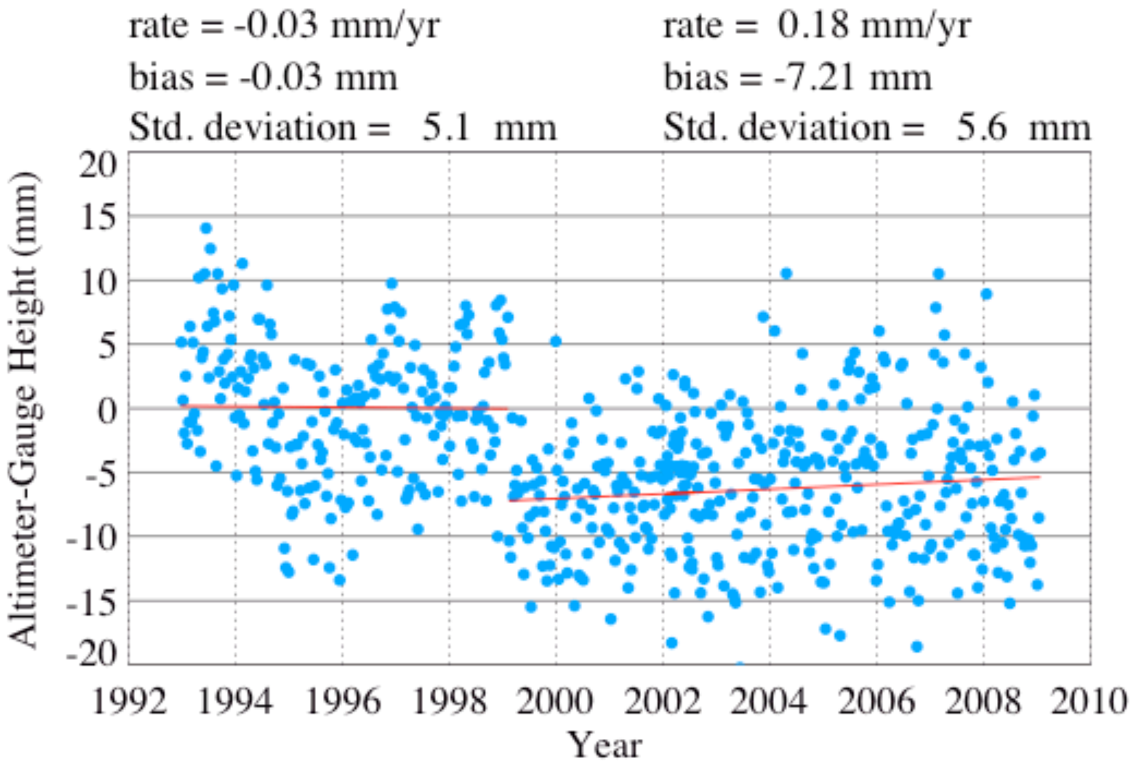

Figure 13: Estimate of TOPEX Side A/B 7.2 mm bias is derived from per cycle mean comparisons of altimeter SSH variations with height variations from 64-site tide gauge network.

To assess the inter-mission consistency and stability of the entire 20-year time series, the TOPEX A/B bias, and the adjustment biases to Jason-1 and Jason-2 that were derived from their verification campaign SSH collinear residuals are applied, and compared against the tide-gauge network as a "single mission" time series. These tide gauge comparisons provided in Figure 14 show per cycle mean differences to be predominantly within a ± 1.0 cm envelope and to have an overall drift rate of -0.1 mm/yr and a standard deviation of the mean differences to the linear fit of 5.8 mm.

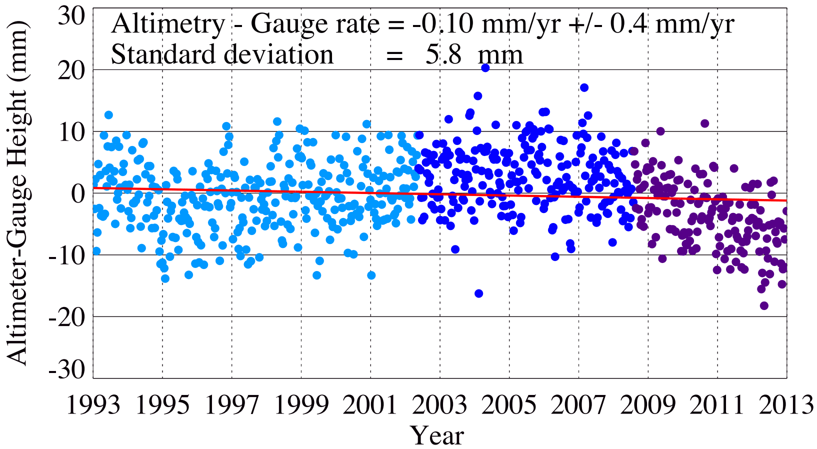

Figure 14: Resultant per cycle comparisons of altimeter derived SSH variations with height variations from 64-site tide gauge network after application of inter-mission biases to form a single adjusted SSH Climate Data Record. TOPEX cycles 11-355 are indicated by light blue dots, Jason-1 cycles 13-239 by dark blue dots, and Jason-2 cycles 1-166 by purple dots.

4.0 Estimation of Global and Regional Mean Sea Level

The geo-referenced structure of the SSH anomaly file enables direct estimates of local mean sea level variations at each reference location. Figure 14 below shows level of agreement of altimetric SSH variations with height variations from Malé tide gauge site in the Maldives Islands. The trend observed from the altimeter minus gauge differences are correlated to the trend observed from DORIS measurements (-0.8 mm/yr ± 1.0 mm/yr) at the site providing insight into the vertical motion of the tide gauge reference (Ray et al., 2010).

Global and regional mean sea level variations derived from the TPJAOS v2.0 product are shown in Figures 16 through 18 below. Details of the derivation of the sea level estimates are provided in Beckley et al., 2007 and 2010. The examples below do have the glacial isostatic adjustment (GIA; Peltier 2009) applied; annual and semi-annual signals are intact in Figure 16, and have been removed in Figures 17 and 18. The edit strategy employed based on the quality flag word bits edited observations where any one of bits 1-4, 9-14 where set to 1, or bits 7 and 8 both set to 1 (see Appendix). Observations where the terrain type is not equal to zero indicating non open-ocean are edited.

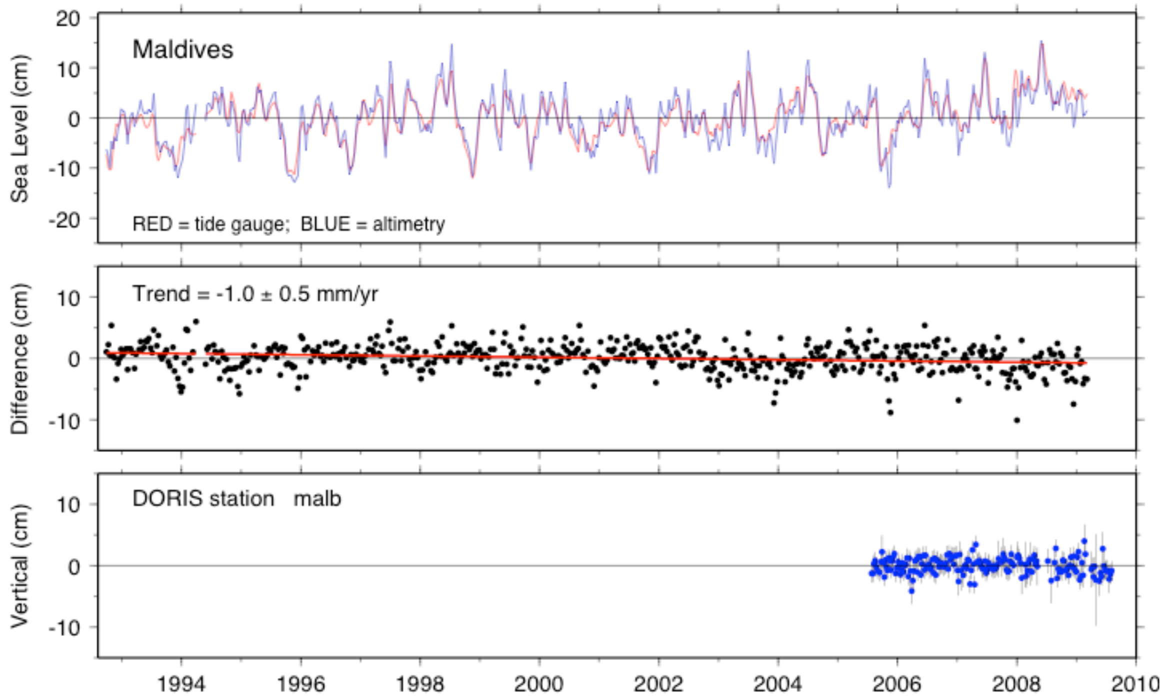

Figure 15: Altimetric and tide-gauge sea levels at Malé in the Maldives Islands (from Ray et. al, 2010). Trend of DORIS observations (blue dots in lower panel) is -0.8 mm/yr yr ± 1.0 mm/yr.

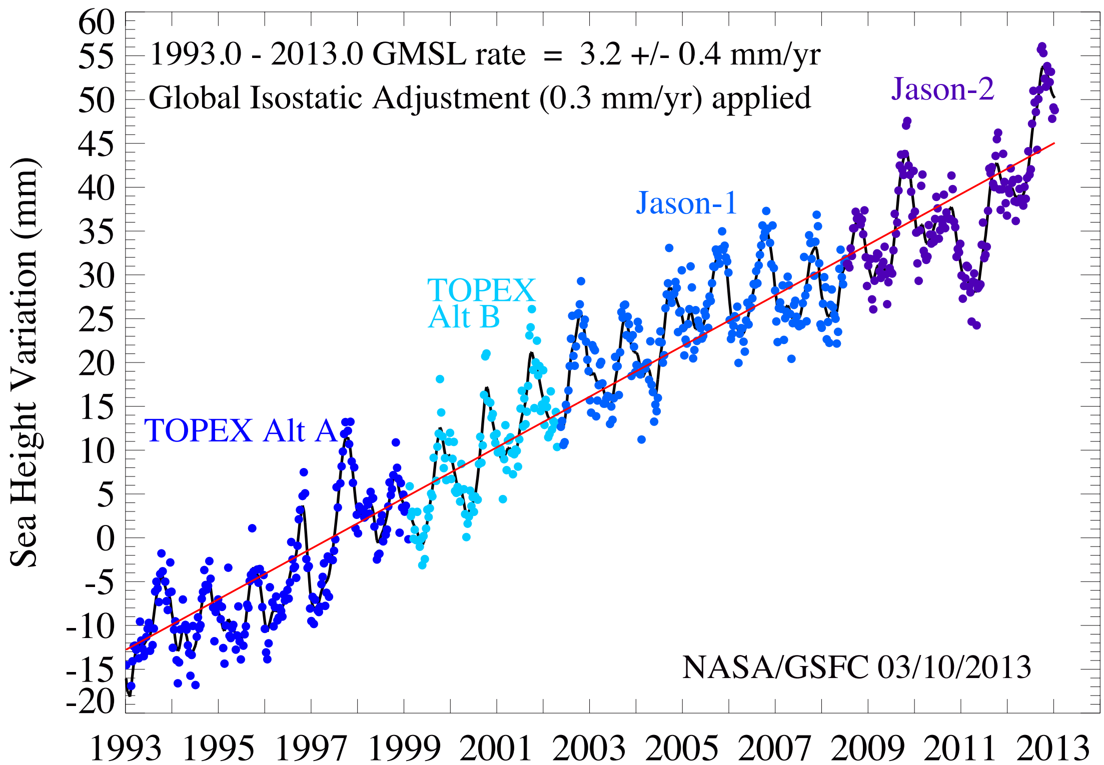

Figure 16: Global mean sea level is estimated at 3.2 ± 0.4 mm/yr (GIA applied) based on SSH variations with respect to 10-year TOPEX mean profile. Sea surface heights are based on cycles 11-748 of TPJAOS v2.0 SSH anomaly product. Black line denotes SSH variation after application of 60-day Hanning filter.

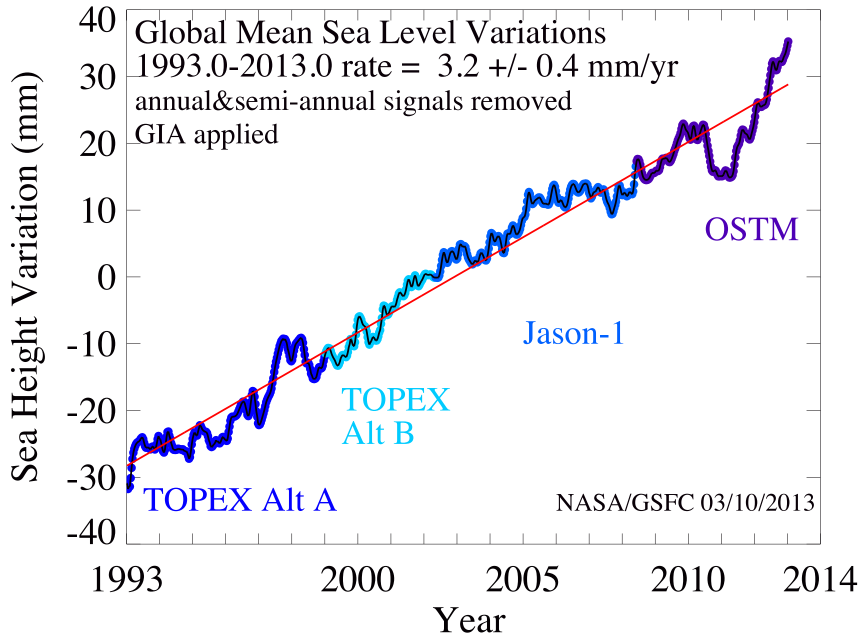

Figure 17: Global mean sea level variations estimated as in Figure 16 with annual and semi-annual signals removed.

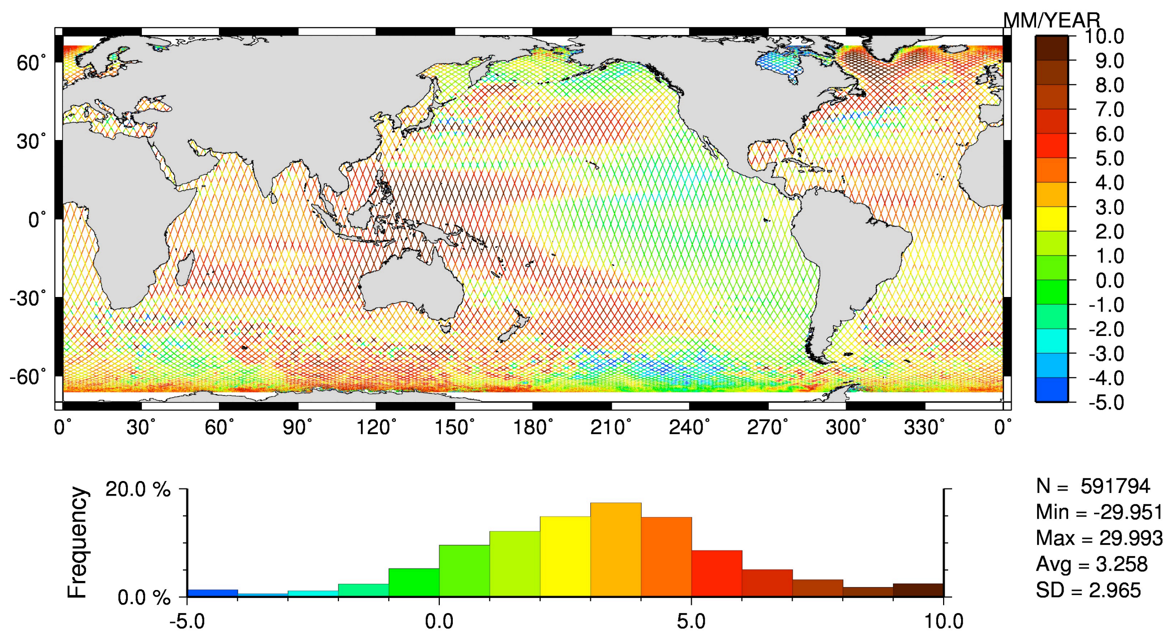

Figure 18: Regional mean sea level variations (GIA applied, annual and semi-annual signals removed) at each geo-referenced location are based on cycles 11-748 of the TPJAOS v2.0 SSH anomaly product.

5.0 References

Ablain, M., A. Cazenave, G. Valladeau, et al., A new assessment of the error budget of global mean sea level rate estimated by satellite altimetry over 1993–2008, Ocean Sci., 5, 193–201, 2009.

Amarouche L., P. Thibaut, O.Z. Zanife, P. Vincent, and N. Steunou. 2004. Improving the Jason-1 ground retracking to better account for attitude effects. *Marine Geodesy*, 27(1-2) :171-197.

Andersen, O. B., and P. Knudsen. 2009. DNSC08 mean sea surface and mean dynamic topography models. *J. Geophys. Res.,* 114, C11001, doi:10.1029/2008JC005179.

Andersen, O. B., 2010. The DTU10 Global Gravity field and Mean Sea Surface – improvements in the Arctic Ocean. Presented at the *2nd International Gravity Field Symposium*, 20-22 September 2010, Fairbanks, Alaska.

Beckley, B.D., N.P. Zelensky, S.B. Luthcke, and P.S. Callahan. 2004. Towards a seamless transition from TOPEX/Poseidon to Jason-1. *Marine Geodesy,* 27, 373-384.

Beckley, B.D., F.G. Lemoine, S.B. Luthcke, R.D. Ray, and N.P. Zelensky. 2007. A reassessment of TOPEX and Jason-1 altimetry based on revised reference frame and orbits. *Geophys. Res. Lett.*, 34, L14608, DOI:10.1029/2007GL030002.

Beckley, B.D., N.P. Zelensky, S.A. Holmes, F.G. Lemoine, R.D. Ray, G.T. Mitchum, S. Desai, S.T. Brown, Assessment of the Jason-2 Extension to the TOPEX/Poseidon, Jason-1 Sea-Surface Height Time Series for Global Mean Sea Level Monitoring, *Marine Geodesy*, 33(S1): 447-471, 2010, Supplemental Issue on OSTM/Jason-2 calibration/validation, Vol. 1, DOI: 10.1080/01490419.2010.491029.

Benada, J. R., 1997. "*PO.DAAC Merged GDR (TOPEX/POSEIDON) Generation B User's Handbook*", Version 2.0, JPL D-11007.

Bertiger W., Desai .S, Dorsey A., Haines B.J., Harvey N., Kuang D., Sibthorpe A., Weiss J.P. (2010) Sub-Centimeter Precision Orbit Determination with GPS for Ocean Altimetry, Marine Geodesy, Vol. 33, Iss. sup1, 2010

Brenner, A. C., C. J. Koblinsky, and B. D. Beckley. 1990. A Preliminary Estimate of Geoid-Induced Variations in Repeat Orbit Satellite Altimeter Observations. *J. Geophys. Res.,* 95(C3), 3033- 3040.

Carrère, L., and F. Lyard. 2003. Modelling the barotropic response of the global ocean to atmospheric wind and pressure forcing. *Geophys. Res. Lett.,* 30(6), art. 1275, DOI:10.1029/2002GL016473.

Cazenave, A., D.P. Chambers, P. Cipollini, L.L. Fu , et al., Sea Level Rise Regional And Global Trends, OCEANOBS2009- Plenary Paper (2009).

Cerri, L., F. Mercier, J.P. Berthias, J.C. Ries, F.G. Lemoine, N.P. Zelensky, et al., Precision orbit determination standards for the Jason series of altimeter missions. Part I, *Marine Geodesy* 33, 2010.

Collard F. and S. Labroue (2004), New Wind Speed Algorithm for Jason-1, Poster presented at the *OSTST Meeting*, November 2004, St Petersburg, Florida, USA.

Chambers, D.P., S.A. Hayes, J.C. Ries, T.J. Urban. 2003. New TOPEX Sea State Bias Models and their Effect on Global Mean Sea Level. *J. Geophys Res*., 108, 3305.

Gaspar, P., F. Ogor, P. Y. Le Traon, and O. Z. Zanife (1994), Estimating the sea state of the TOPEX and Poseidon altimeters from crossover differences, J. Geophys. Res., 99, 24,981 – 24,994.

Gaspar, P., and J.-P. Florens. 1998. Estimation of the sea state bias in radar altimeter measurements of sea level: Results from a new nonparametric method. *J. Geophys. Res.* 103:15803-15814.

Gaspar, P., S. Labroue, F. Ogor, G. Lafitte, L. Marchal, and M. Rafanel. 2002. Improving nonparametric estimates of the sea state bias in radar altimeter measurements of sea level. *J. Atmos. Oceanic Technol.* 19:1690-1707.

Goiginger, H., et al. (2011), The combined satellite-only global gravity field model GOCO02S, Geophysical Research Abstracts, 13, EGU2011–10,571.

Gourrion, J., D. Vandemark, S. Bailey, B. Chapron, G. P. Gommenginger, P. G. Challenor, and M. A. Srokosz (2002), A two-parameter wind speed algorithm for Ku-band altimeters, J. Atmos. Oceanic Technol., 19, 2030 – 2048.

Labroue, S., P. Gaspar, J. Dorandeu, O.Z. Zanife, F. Mertz, P. Vincent, and D. Choquet. 2004. Nonparametric estimates of the sea state bias for the Jason-1 radar altimeter. *Mar. Geod.* 27:453-481.

Lemoine, F.G., N.P. Zelensky, D.S. Chinn, D.E. Pavlis, D.D. Rowlands, B.D. Beckley, S.B. Luthcke, P. Willis, M. Ziebart, A. Sibthorpe, J. Boy, V. Luceri, Towards development of a consistent orbit series for TOPEX, Jason-1, and Jason-2, Adv. Space Research, 46 (2010) 1513-1540, doi: 10.1016/j.asr.2010.05.007

Lemoine, F.G., N. P. Zelensky, S. Melachroinos, D. S. Chinn, D. E. Pavlis, D.D. Rowlands, B.D. Beckley, R.D. Ray, S. B. Luthcke, Improved Orbit Standards for Altimeter Satellite POD at GSFC, POD Splinter oral presentation 2012 OSTST, Venice Italy.

Lyard, F., F. Lefevre, T. Letellier, and O. Francis, "Modeling the global ocean tides: Insights from FES2004", Ocean Dyn., 56, 394–415, 2006.

Marshall, J.A., Zelensky, N.P., Luthcke, S.B., Rachlin, K.E., Williamson R.G. (1995), The temporal and spatial characteristics of TOPEX/Poseidon radial orbit error*, J. Geophys Res.*, *100(C12)*, pp. 25331-25352.

Mitchum, G.T. 2000. An improved calibration of satellite altimetric heights using tide gauge sea levels with adjustment for land motion. *Marine Geodesy*, 23, 145-166.

Leuliette, E.W., and R. Scharroo, Integrating Jason-2 into a Multiple-Altimeter Climate Data Record, *Marine Geodesy*, 33(S1): 504-517, 2010, Supplemental Issue on OSTM/Jason-2 calibration/validation, Vol. 1, DOI: 10.1080/01490419.2010.487795.

Nerem, R.S., D.P. Chambers, C. Choe, G.T. Mitchum, Estimating Mean Sea Level Change from the TOPEX and Jason Altimeter Missions, *Marine Geodesy*, 33(S1): 435-446, 2010, Supplemental Issue on OSTM/Jason-2 calibration/validation, Vol. 1, DOI: 10.1080/01490419.2010.491031.

OSTM/Jason-2 products handbook, Issue 1 rev 8, December 1, 2011. SALP-MU-M-OP-15815-CN(CNES), EUM/OPS-JAS/MAN/08/0041 (EUMETSAT), OSTM-29-1237 (JPL), Polar Series/OSTM J400 (NOAA/NESDIS).

Peltier, W. R., 2009. Closure of the budget of global sea level rise over the GRACE era: The importance and magnitude of the required corrections for global glacial isostatic adjustment, Quat. Sci. Rev. 17–18:1658–1674, doi:10.1016/j.quascirev.2009.04.004.

Picot, N., K. Case, S. Desai, and P. Vincent. 2008. *AVISO and PODAAC User Handbook. IGDR and GDR Jason Products, Edition 4.0*. SMM-MU-M5-OP-13184-CN (**AVISO**), JPL D-21352 (**PODAAC**).

Ponte, R. M. and R. D. Ray, "Atmospheric pressure corrections in geodesy and oceanography: a strategy for handling air tides," Geophysical Research Letters, 29(24), 2153, 2002.

Ray, R. D. and D. E. Cartwright, "Satellite altimeter observations of the Mf and Mm ocean tides, with simultaneous orbit corrections," in Gravimetry and Space Techniques Applied to Geodynamics and Ocean Dynamics, pp. 69-78, American Geophysical Union, Washington, 1994.

Ray, R. D. and R. M. Ponte, "Barometric tides from ECMWF operational analyses," Annales Geophysicae, 21, 1897-1910, 2003.

Schrama, E. J. O. and R. D. Ray, "A preliminary tidal analysis of TOPEX/Poseidon altimetry," Journal of Geophysical Research, 99, 24799-24808, 1994.

Ray, R.D. 1999. A global ocean tide model from TOPEX/Poseidon altimetry: GOT99.2, NASA TM-1999-209478, NASA Goddard Space Flight Center, September 1999 (Update).

Ray, R.D., B.D. Beckley, F.G. Lemoine. Vertical crustal motion derived from satellite altimetry and tide gauges, and comparisons with DORIS measurements. Adv. Space Research, 45 (2010) 1510-1522, doi: 10.1016/j.asr.2010.02.020

TOPEX Ground System Science Algorithm Specification, JPL D-7075, Rev. A, Change 1; April 25, 1991.

Tran, N., Phillips, E. Bronner, and N. Picot, Impact of GDR_D standards on SSB corrections, Ocean Surface Topography Science Working Team Meeting, Venice, Italy, 2012. http://www.aviso.oceanobs.com/fileadmin/documents/OSTST/2012/oral/02_friday_28/01_instr_processing_I/01_IP1_Tran.pdf

Tran, N., S. Labroue, S. Phillips, E. Bronner, and N. Picot, Overview and Update of the Sea State Bias Corrections for the Jason-2, Jason-1, and TOPEX Missions. *Mar. Geod.* 33(S1): 348-362, 2010. DOI: 10.1080/01490419.2010.487788

Wöppelmann, G., C. Letetrel, A. Santamaria, M.-N. Bouin, X. Collilieux, Z. Altamimi, S.D.P. Williams, B. Martin Miguez, 2009. Rates of sea-level change over the past century in a geocentric reference frame. Geophys. Res. Lett. 36, L12607, 2009.

Zelensky, N.P., F.G. Lemoine, M. Ziebart, A. Sibthorpe, P. Willis, B.D. Beckley, S.M. Klosko, D.S. Chinn, D.D. Rowlands, S.B. Luthcke, D.E. Pavlis, V. Luceri, DORIS/SLR POD modeling improvements for Jason-1 and Jason-2, Adv. Space Research, 46(12), 1541-1558, 2010. doi: 10.1016/j.asr.2010.05.008

Zelensky, N.P., F. G. Lemoine, B. Beckley, D. S. Chinn, S. Melachroinos, S. B. Luthcke G. Mitchum, O. Bordyugov, Improved Modelling of Time-Variable Gravity for Altimeter Satellite POD, POD Splinter poster 2012 OSTST, Venice Italy.

Appendix I: Quality Flag Bit Distributions

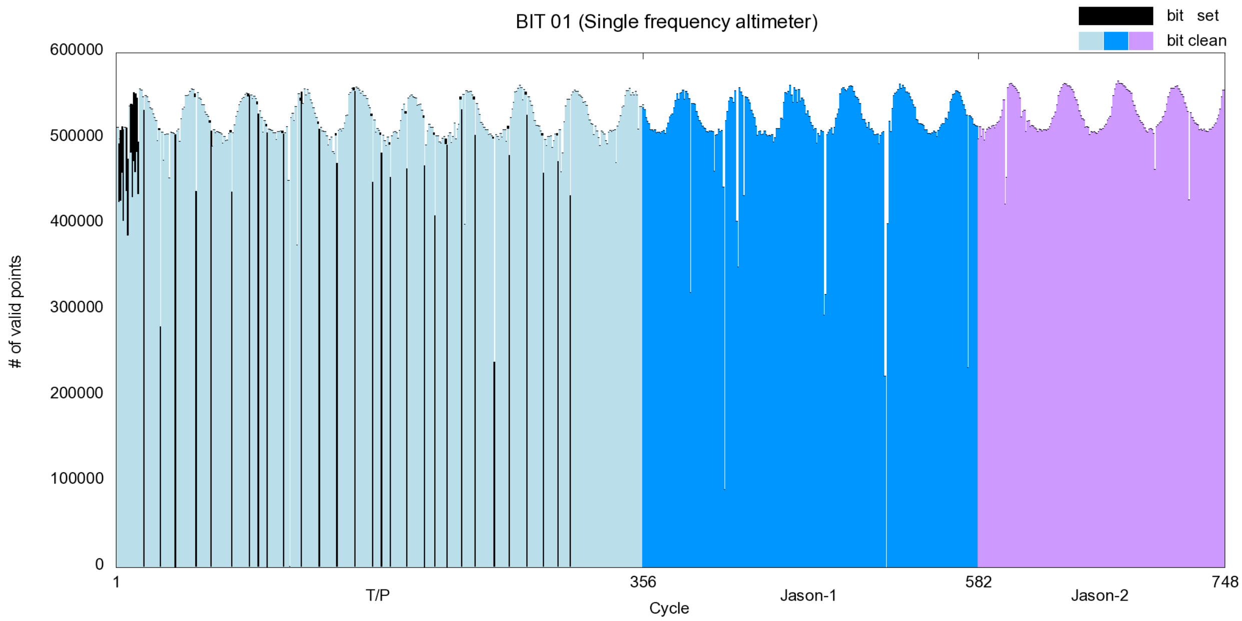

Figure A-1: Quality flag word Bit #1 when set to 1 indicates Poseidon-1 (single frequency) altimeter observations.

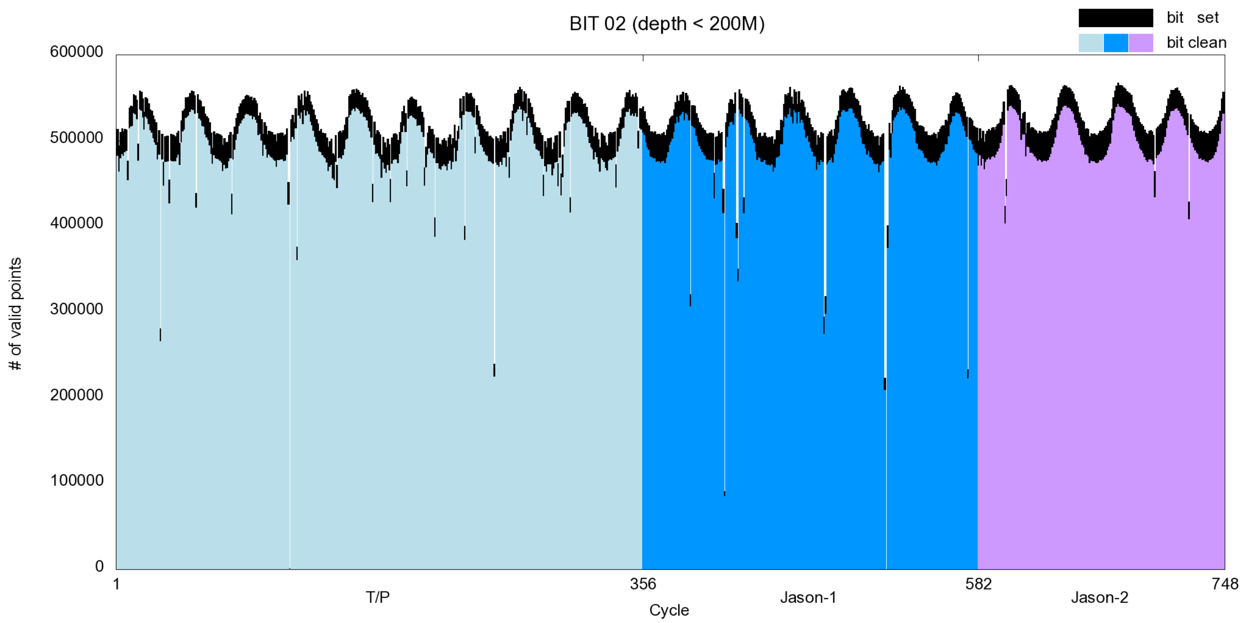

Figure A-2: Quality flag word Bit #2 when set to 1 indicates locations where ocean depth < 200 m.

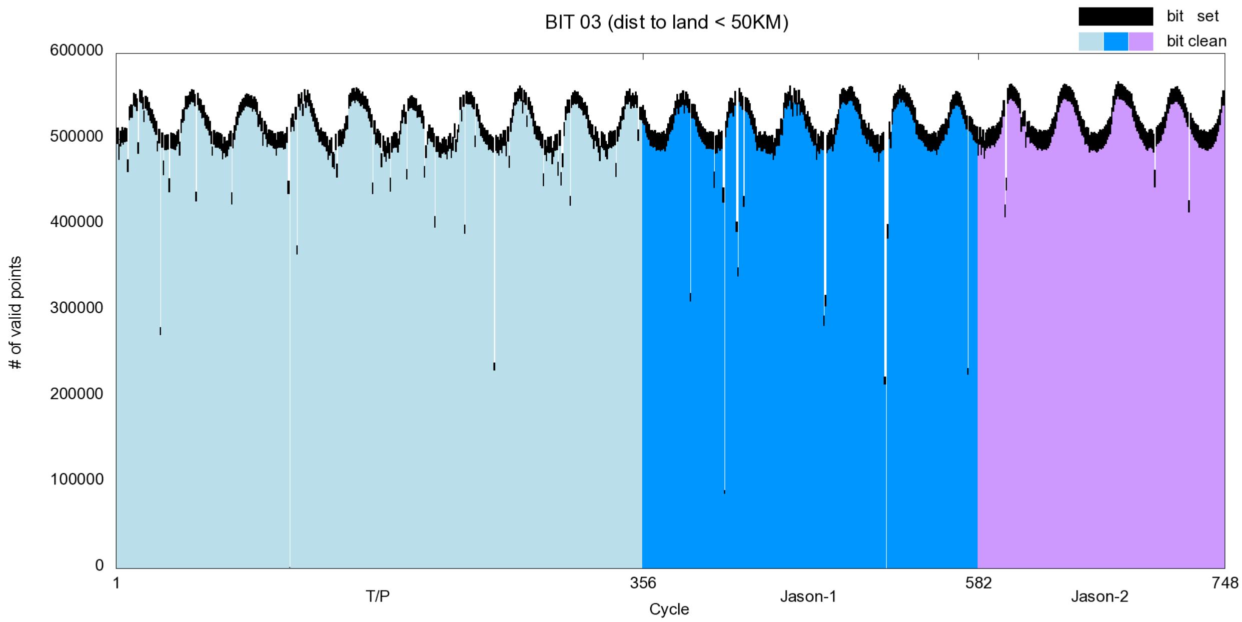

Figure A-3: Quality flag word bit #3 when set to 1 indicates locations within 50 km to coastline.

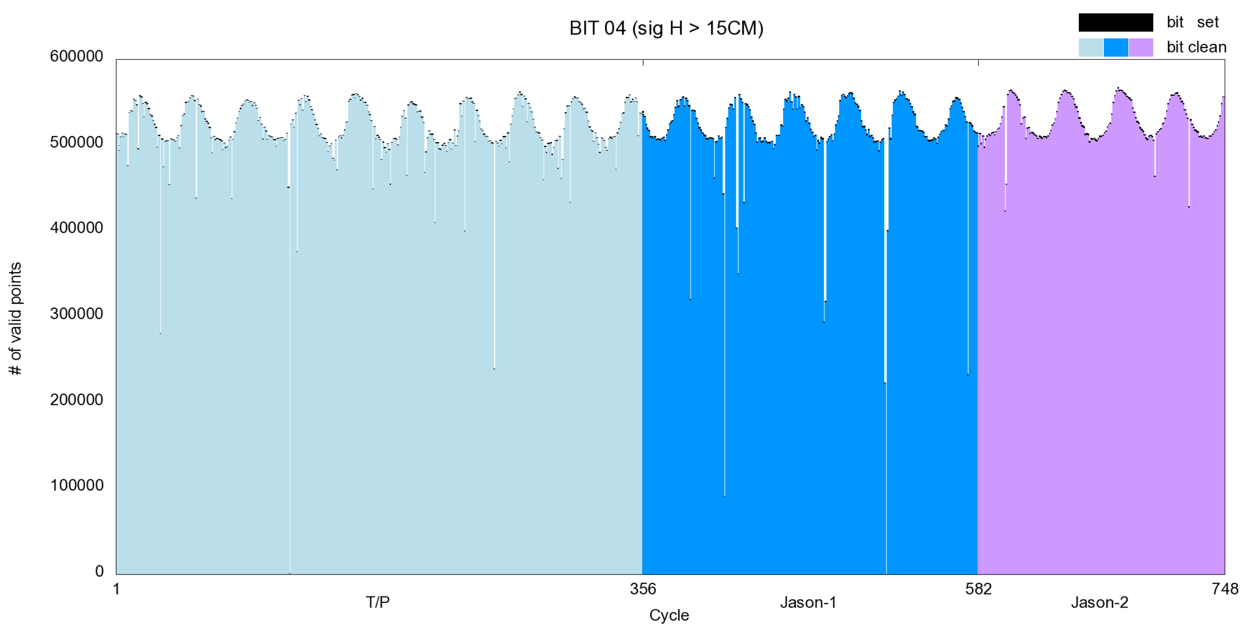

Figure A-4: Quality flag word bit #4 when set to 1 identifies 1Hz SSH measurements with standard deviation of high rate SSH residuals with respect to 1Hz "average" is grater than 15 cm (20 cm for Poseidon-1).

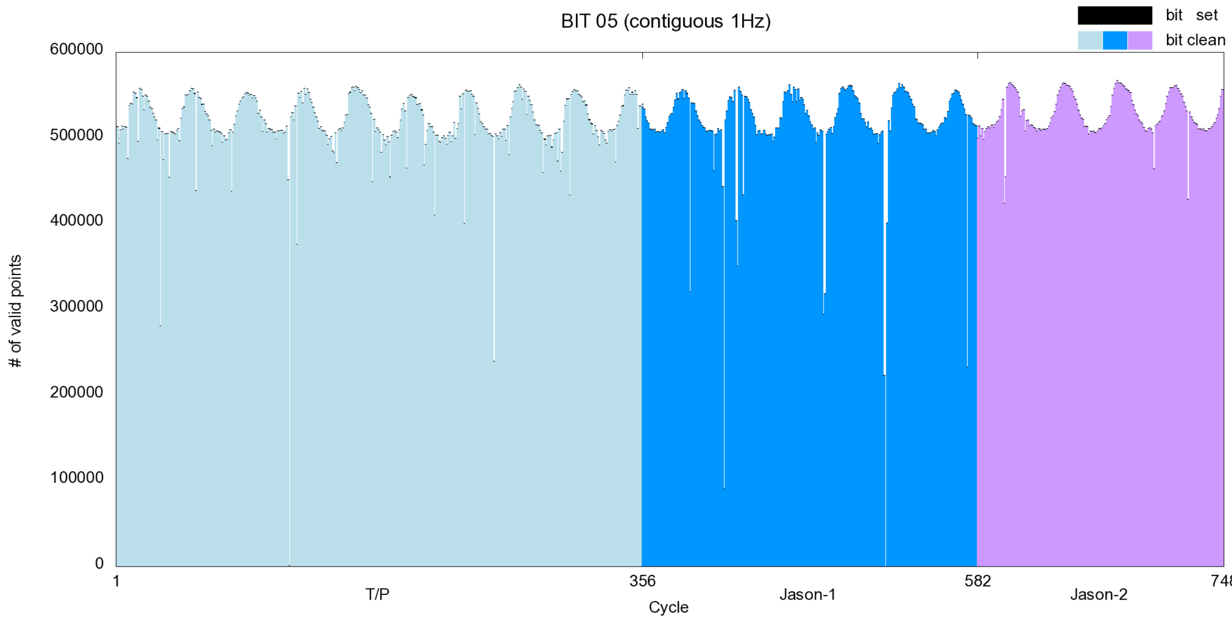

Figure A-5: Quality flag word bit #5 when set to 1 identifies 1Hz geo-referenced SSH values not derived from a nominal contiguous pair of high rate SSH measurements.

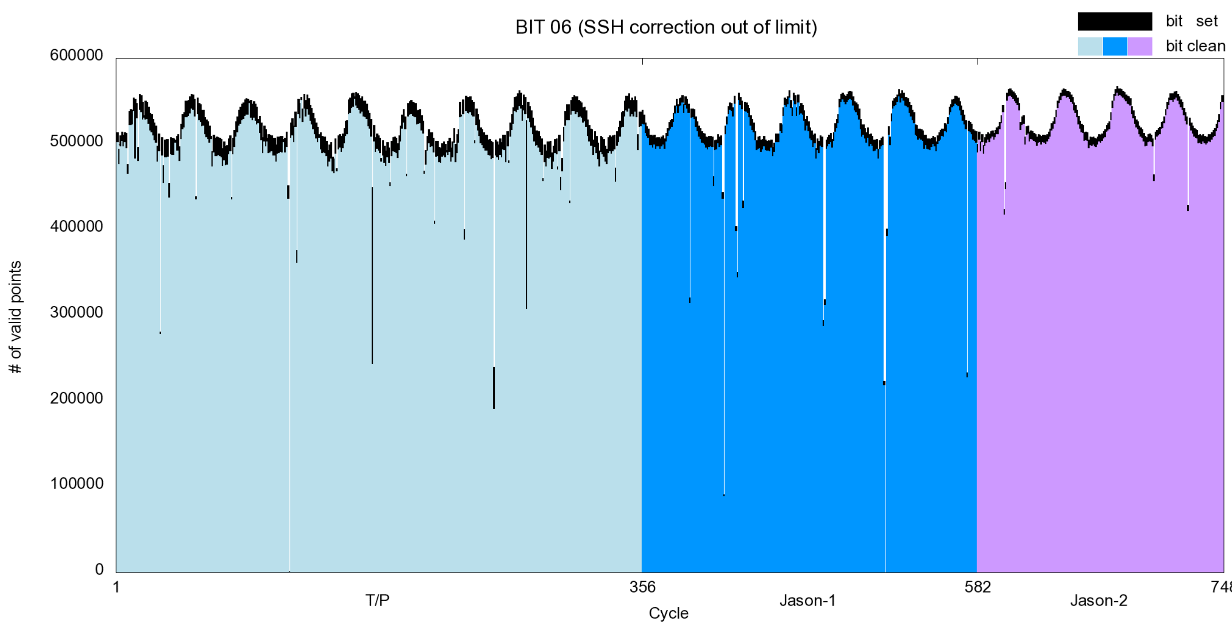

Figure A-6: Quality flag word bit #6 when set to 1 identifies valid (not equal to 32767) 1Hz geo-referenced SSH with one or more range or geophysical corrections outside nominal limits (see table 2).

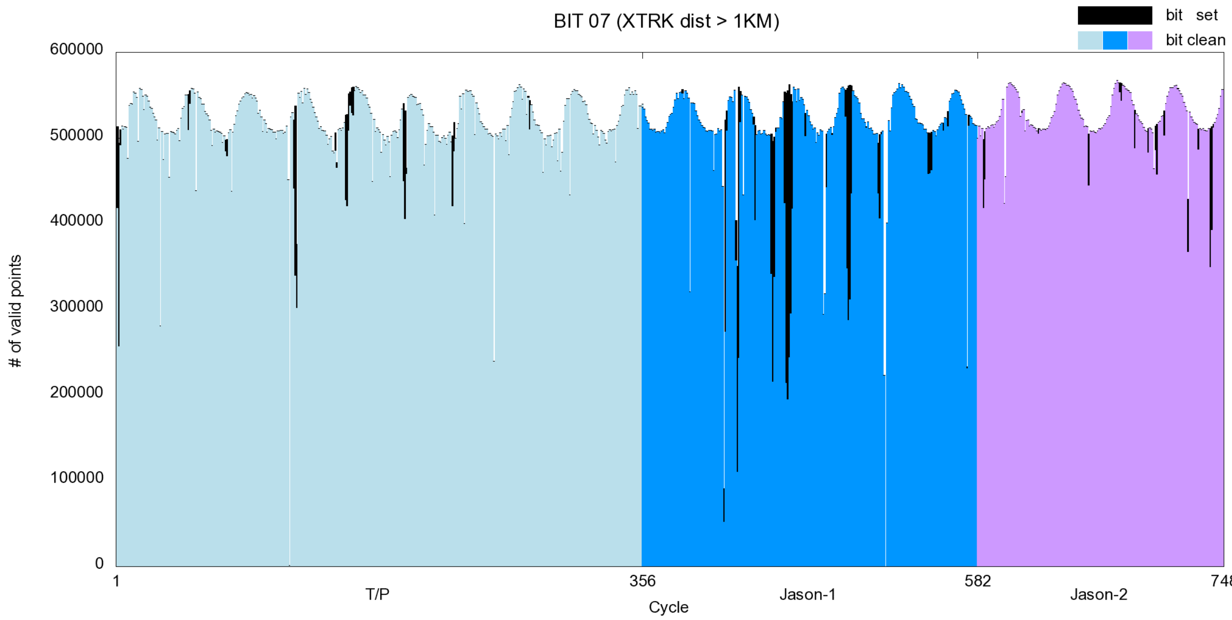

Figure A-7: Quality flag word bit #7 when set to 1 identifies locations with a cross-track distance > 1 km with respect to reference orbit.

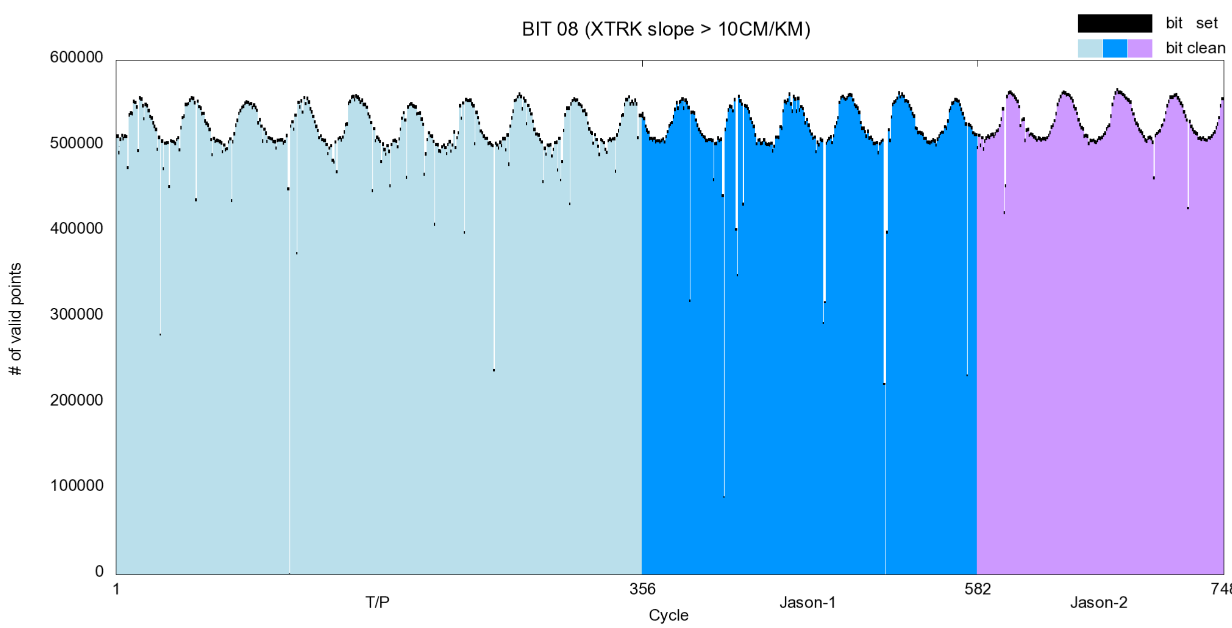

Figure A-8: Quality flag word bit #8 when set to 1 identifies locations with cross track geoid gradients exceeding 10 cm/km.

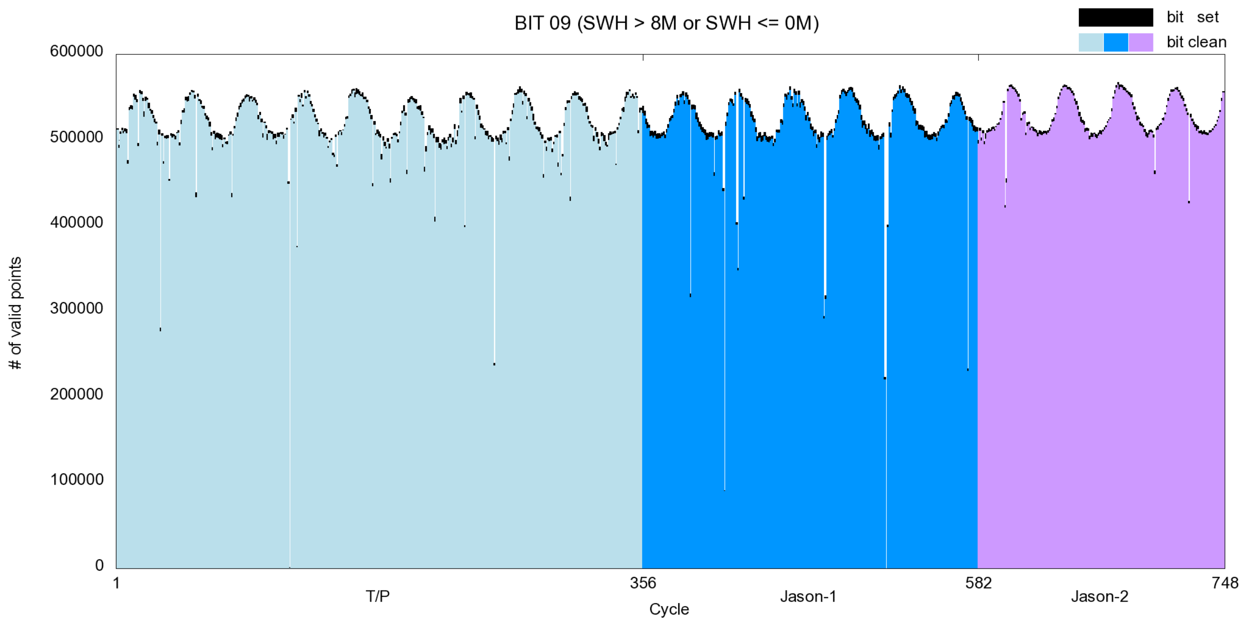

Figure A-9: Quality flag word bit #9 when set to 1 indicates SSH measurements at high sea states with SWH_Ku greater than 8.0 m, less than or equal to 0m.

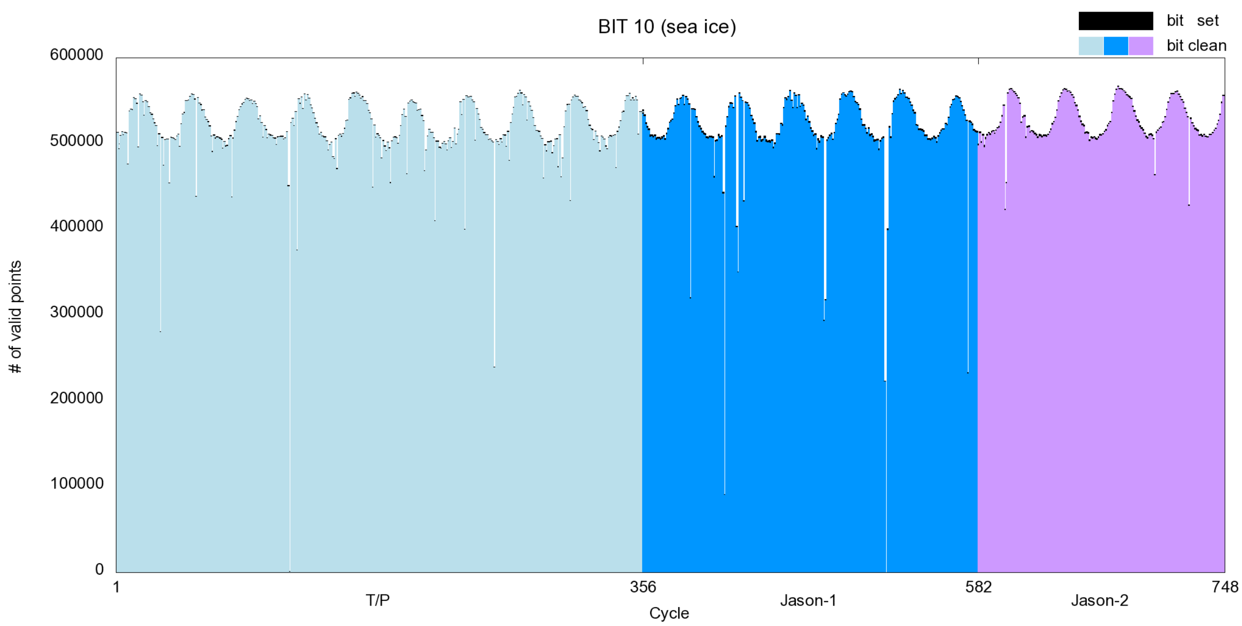

Figure A-10: Quality flag word bit #10 when set to 1 indicates observations with possible contamination of SSH estimate from presence of sea ice.

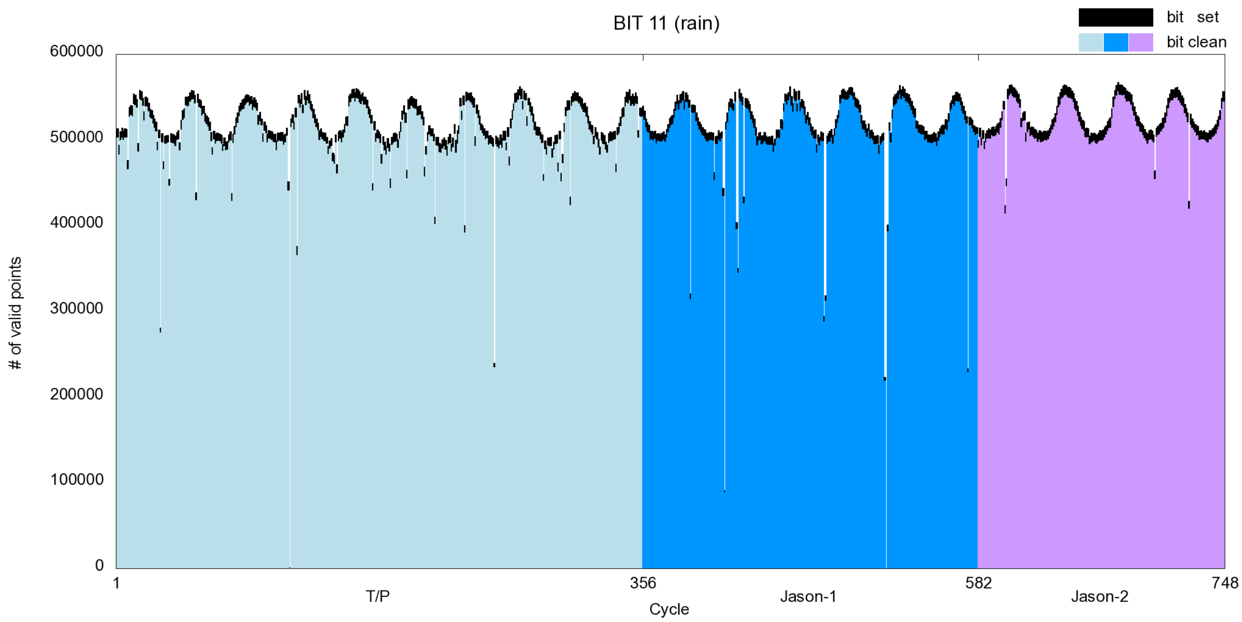

Figure A-11: Quality flag word bit 11 when set to 1 indicates observations with possible contamination of SSH estimate due to presence of rain. Current algorithm specifications for rain/sea ice detection are in Appendix II below.

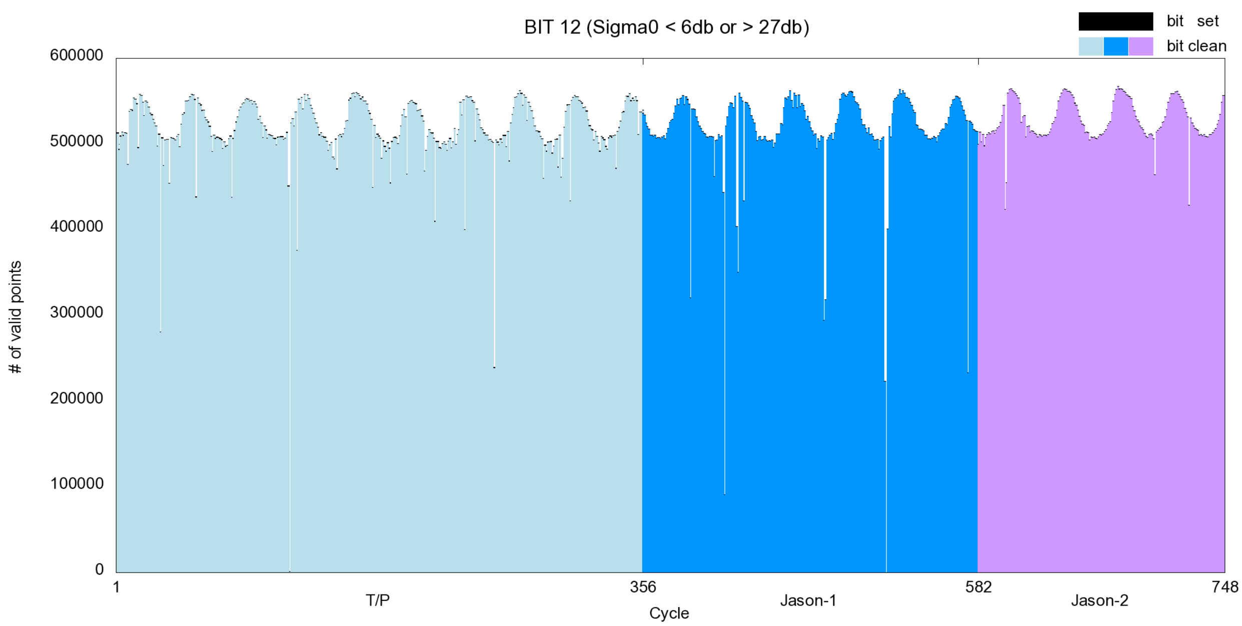

Figure A-12: Quality flag word bit #12 when set to 1 identifies observations with backscatter coefficients outside nominal range indicating high wind conditions or possible land/ice contamination.

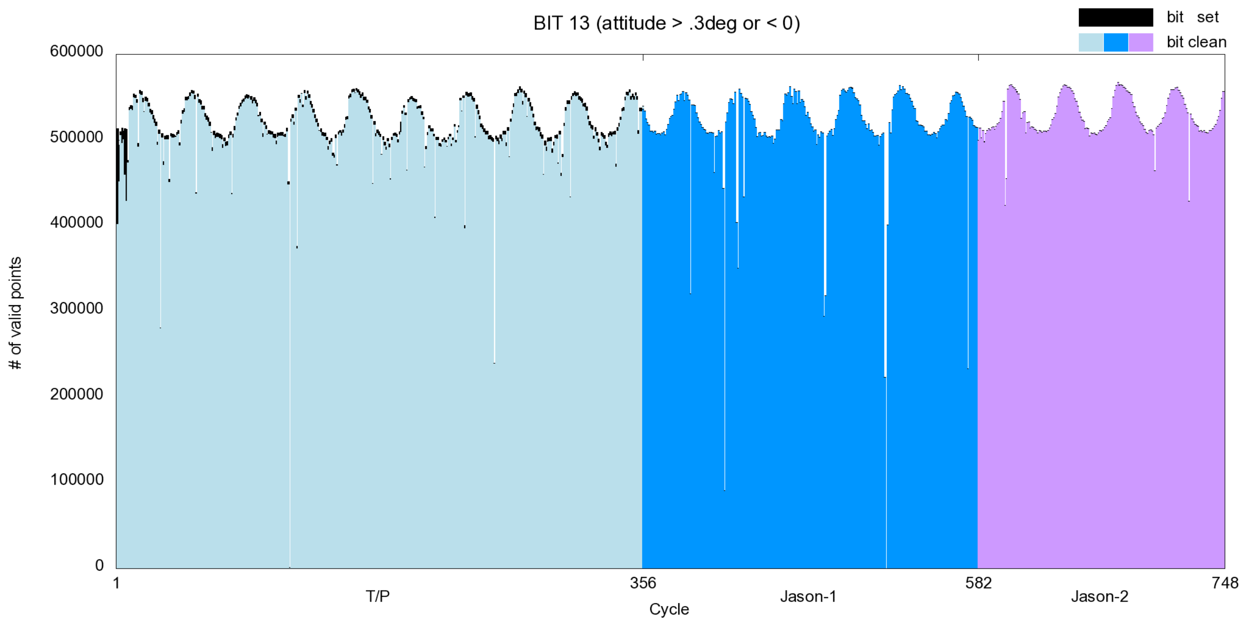

Figure A-13: Quality flag word bit #13 when set to 1 identifies observations when the attitude_waveform is outside nominal range limits.

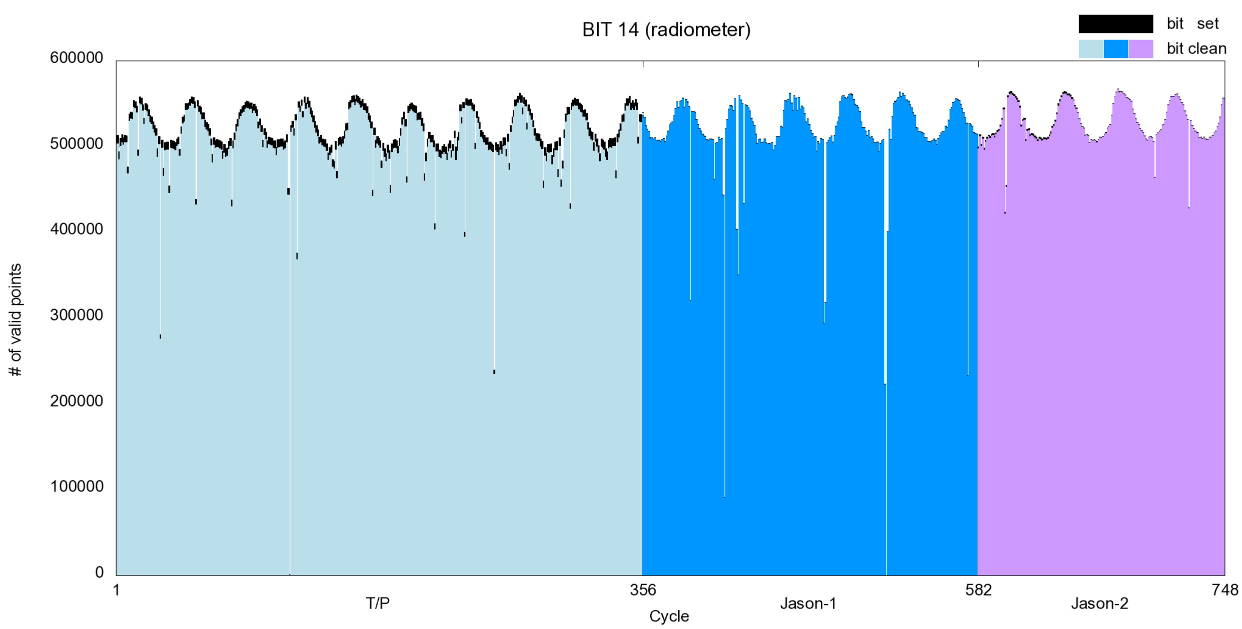

Figure A-14: Quality flag word bit #14 when set to 1 indentifies observations where the radiometer measurement is believed to be suspect.

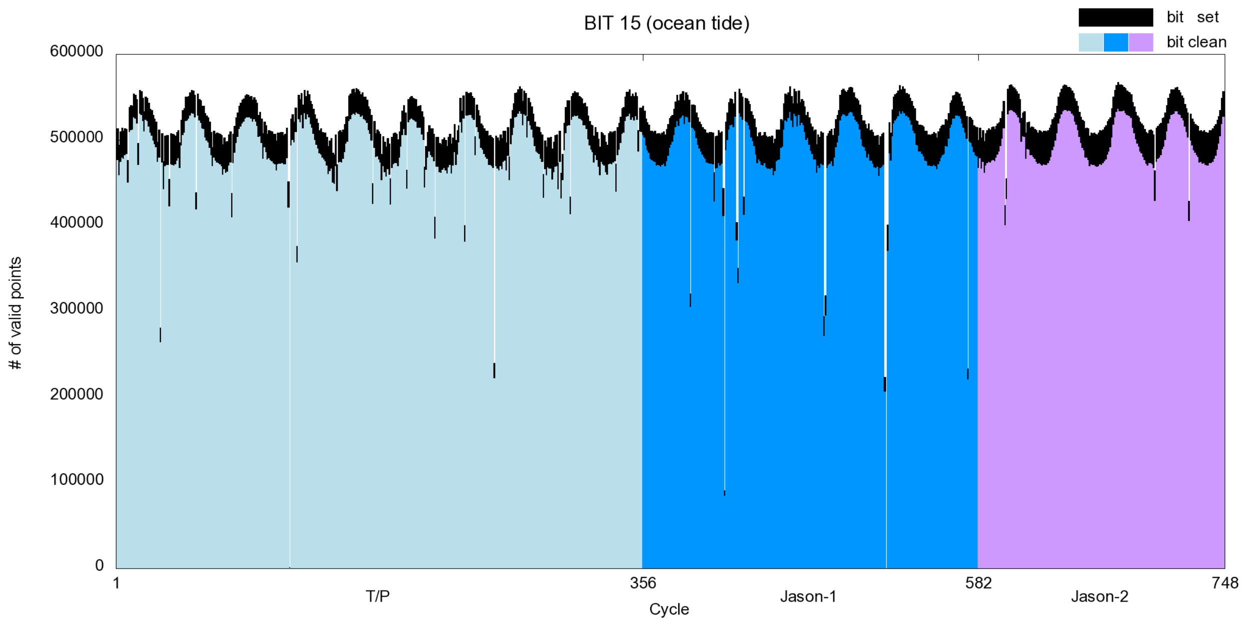

Figure A-15: Quality flag word bit #15 when set to 1 identifies coastal locations where the mean GOT4.8/FES04 ocean tide correction differs by more than 2.0 cm (see figure 20).

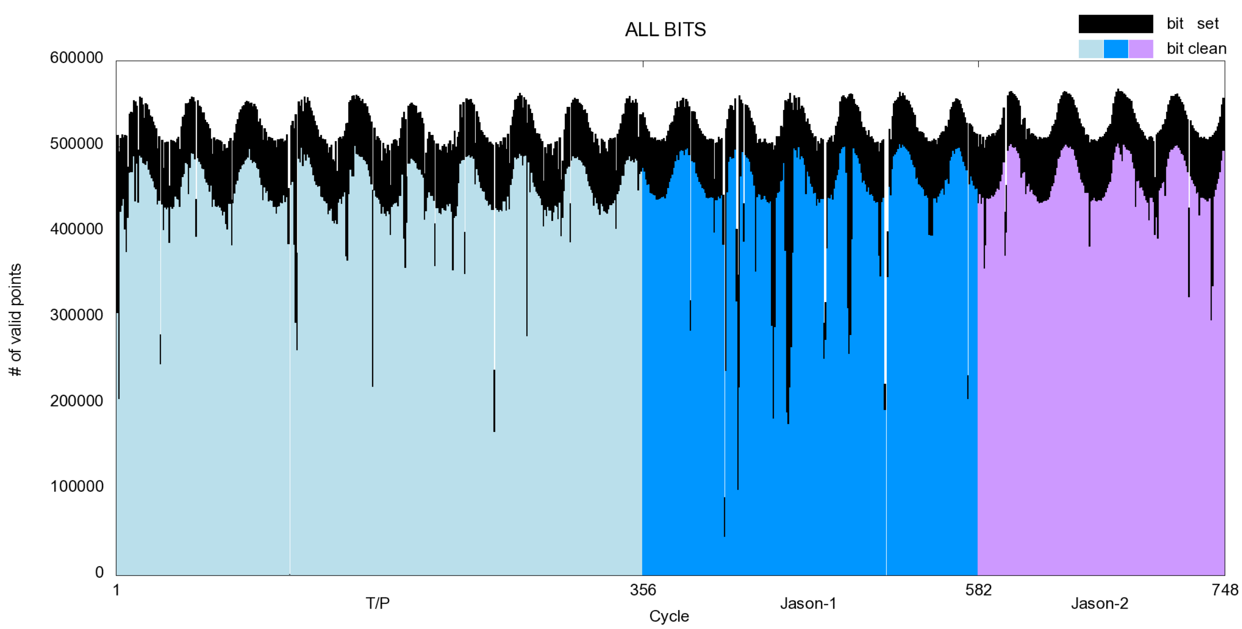

Figure A-16: An edit strategy that requires all bits set to 0 (except bit #1 to retain Poseidon-1 data) will result in ~ 10 % data loss.

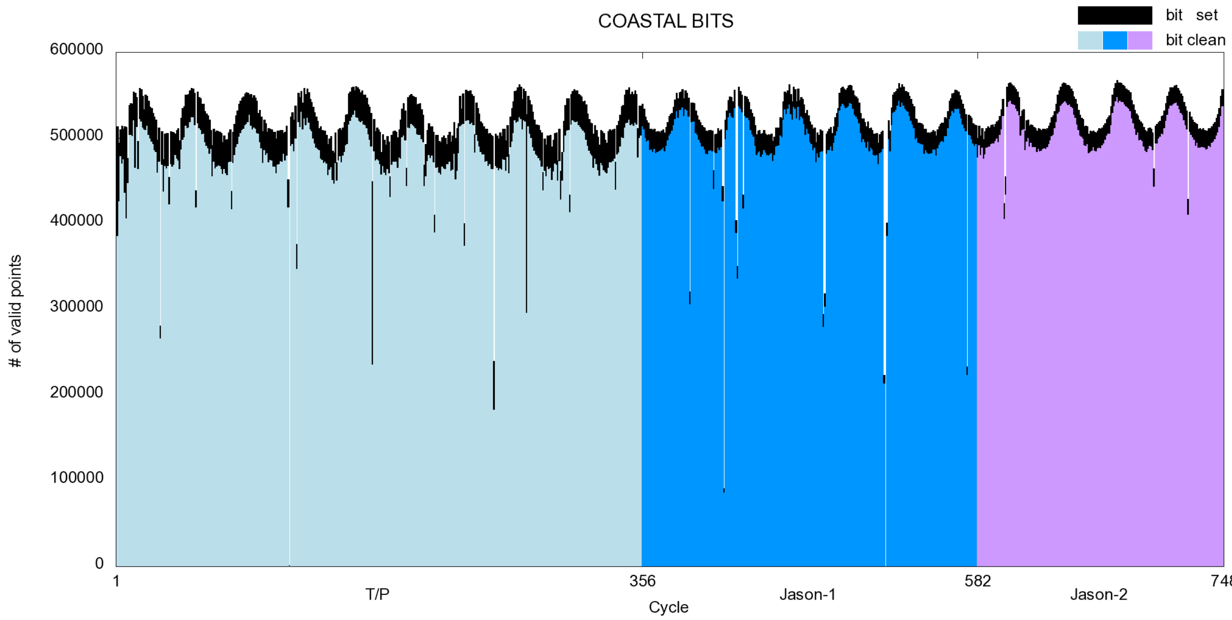

Figure A-17: Edit strategy as above except coastal observations are retained (bits 2,3, and 15) and both bits 7&8 in combination must be set, resulting in ~ 5 % data loss.

Appendix II: Sea State Bias Specifications

Jason-2: ssb_col_J2_Ku_mle4_1_36_v2012ostst.rs (Tran et al., 2012.)

Jason-1: ssb_col_J1_1_111_v2012ostst.rs (Tran et al., 2010)

TOPEX Side A: ssb_col_TPmgdr_021_131_v2009.rs (Tran et al., 2010)

TOPEX Side B: ssb_col_TPmgdr_240_350_v2009.rs (Tran et al., 2010)